Chemoprevention by nonsteroidal anti-inflammatory drugs eliminates oncogenic intestinal stem cells via SMAC-dependent apoptosis

Wei Qiu[a], Xinwei Wang[a], Brian Leibowitz[a], Hongtao Liu[a], Nick Barker[b], Hitoshi Okada[c], Naohide Oue[d], Wataru Yasui[d], Hans Clevers[b], Robert E. Schoen[a], Jian Yu[a,1], and Lin Zhang[a,1]

[a]University of Pittsburgh Cancer Institute and Departments of Pharmacology and Chemical Biology, Pathology, and Medicine, University of Pittsburgh School of Medicine, Pittsburgh, PA 15213; [b]The Hubrecht Institute for Developmental Biology and Stem Cell Research, 3584 CT, Utrecht, The Netherlands; [c]The Campbell Family Institute for Breast Cancer Research, Ontario Cancer Institute, University Health Network, Toronto, ON, Canada M5G 2C1; and [d]Department of Molecular Pathology, Hiroshima University Graduate School of Biomedical Sciences, Hiroshima 734-8553, Japan

Edited* by Bert Vogelstein, The Sidney Kimmel Comprehensive Cancer Center at Johns Hopkins, Baltimore, MD, and approved October 6, 2010 (received for review July 18, 2010)

Nonsteroidal anti-inflammatory drugs (NSAIDs) such as sulindac effectively prevent colon cancer in humans and rodent models. However, their cellular targets and underlying mechanisms have remained elusive. We found that dietary sulindac induced apoptosis to remove the intestinal stem cells with nuclear or phosphorylated β-catenin in $APC^{Min/+}$ mice. NSAIDs also induced apoptosis in human colonic polyps and effectively removed cells with aberrant Wnt signaling. Furthermore, deficiency in SMAC, a mitochondrial apoptogenic protein, attenuated the tumor-suppressive effect of sulindac in $APC^{Min/+}$ mice by blocking apoptosis and removal of stem cells with nuclear or phosphorylated β-catenin. These results suggest that effective chemoprevention of colon cancer by NSAIDs lies in the elimination of stem cells that are inappropriately activated by oncogenic events through induction of apoptosis.

Prevention of human cancers by using chemical agents or dietary manipulation represents a promising anticancer strategy (1, 2). Widely used nonsteroidal anti-inflammatory drugs (NSAIDs) such as sulindac and aspirin effectively prevent colon cancer in humans and rodent models (3, 4). However, their cellular targets and underlying mechanisms have remained elusive. Colorectal tumorigenesis is initiated by genetic alterations in the *APC* tumor suppressor pathway through Wnt signaling, leading to accumulation of β-catenin and its subsequent nuclear translocation (5). This process has been largely recapitulated in animal models such as $APC^{Min/+}$ mice, which contain an *APC* mutation and exhibit intestinal adenoma formation (6). Emerging evidence suggests that initial neoplastic proliferation in $APC^{Min/+}$ mice impinges upon loss of *APC* in intestinal stem cells (7, 8), including crypt base columnar (CBC) cells near the crypt bottom, as well as those located in position 4–6 (+4) counting from the crypt bottom (9). Several intestinal stem cell markers have been identified, such as Lgr5 (10), Bmi1 (8), and OLFM4 (11).

Substantial evidence indicates that the chemopreventive effects of NSAIDs are mediated by induction of apoptosis, a safeguard mechanism protecting against neoplastic transformation (12, 13). Our previous work established that NSAIDs induce mitochondria- and Bax-dependent apoptosis in colon cancer cells (14), and that SMAC (second mitochondria-derived activator of caspase), a mitochondrial apoptogenic protein (15), is an essential downstream mediator of Bax in NSAID-induced apoptosis (16, 17). In this study, we investigated the role of intestinal stem cell apoptosis in chemoprevention by NSAIDs. Our data suggest a critical role of SMAC-mediated apoptosis in removing early neoplastic stem cells in cancer chemoprevention by NSAIDs.

Results

Sulindac Treatment Induced Apoptosis in Intestinal Stem Cells of $APC^{Min/+}$ Mice. Dietary supplementation with NSAIDs such as sulindac for several months prevents adenoma formation in the small intestine of $APC^{Min/+}$ mice (18). To study the role of apoptosis in chemoprevention by NSAIDs, we first determined the time window for analyzing sulindac-induced apoptosis in $APC^{Min/+}$ mice because of the rapid and transient nature of apoptotic events. We found that sulindac given for only 1 wk markedly induced apoptosis detected by TUNEL staining in the small intestinal crypts of $APC^{Min/+}$ mice, with 22.1% of crypts containing at least one TUNEL-positive cell, compared with only 4.0% in mice receiving control diet (Fig. 1*A*). Importantly, this short exposure reduced the number of macroadenomas by 66.7% (Fig. 1*B*), consistent with observations made by others (19). Sulindac treatment for 2 wk or longer further decreased polyp numbers (Fig. S1*A*). However, TUNEL staining detected little apoptosis at 2 wk or later after treatment (Fig. 1*A* and Fig. S1*B*), suggesting that most of the apoptosis had occurred earlier. As previously shown (20), sulindac treatment did not significantly affect polyp formation in the colon of $APC^{Min/+}$ mice. These observations indicate that sulindac rapidly induces apoptosis in the small intestine of $APC^{Min/+}$ mice, and this early apoptosis may be responsible for effective chemoprevention. Therefore, 1-wk sulindac treatment was chosen for most of the subsequent experiments.

In light of recent reports that *APC* loss in intestinal stem cells efficiently promotes adenoma formation (7, 8), we further determined the types of cells undergoing apoptosis in $APC^{Min/+}$ mice following 1 wk of sulindac treatment. Remarkably, a majority of TUNEL-positive cells were the wedge-shaped CBC cells (62.7%) and +4 cells (27.5%), whereas apoptotic cells were rare (<10%) at higher positions in the crypts (Fig. 1 *C* and *D* and Fig. S2). Upon introducing the Lgr5-EGFP lineage marking allele (10) into $APC^{Min/+}$ mice, we found that sulindac treatment induced apoptosis in Lgr5-expressing cells of *Lgr5-EGFP*/$APC^{Min/+}$ mice, but not WT mice (Fig. 1 *C* and *E* and Fig. S3). The fraction of Lgr5-positive crypts containing one or more TUNEL-positive cells increased from 4.32% in the control mice to 17.60% in the sulindac-treated mice (Fig. 1*E*). We confirmed that the Lgr5-marked CBC cells and apoptotic cells at the crypt base were interspersed between MMP7-positive Paneth cells (Fig. 1*C* and Figs. S3*B* and S4) (21). Active caspase 3 staining verified the induction of apoptosis in these cells (Fig. 1*F* and Fig. S3*C*). Interestingly, apoptotic CBC cells were found to be clustered in

Author contributions: W.Q., J.Y., and L.Z. designed research; W.Q., X.W., B.L., and H.L. performed research; N.B., H.O., N.O., W.Y., H.C., and R.E.S. contributed new reagents/analytic tools; W.Q., J.Y., and L.Z. analyzed data; and W.Q., J.Y., and L.Z. wrote the paper.

The authors declare no conflict of interest.

*This Direct Submission article had a prearranged editor.

[1]To whom correspondence may be addressed. E-mail: zhanglx@upmc.edu or yuj2@upmc.edu.

This article contains supporting information online at www.pnas.org/lookup/suppl/doi:10.1073/pnas.1010430107/-/DCSupplemental.

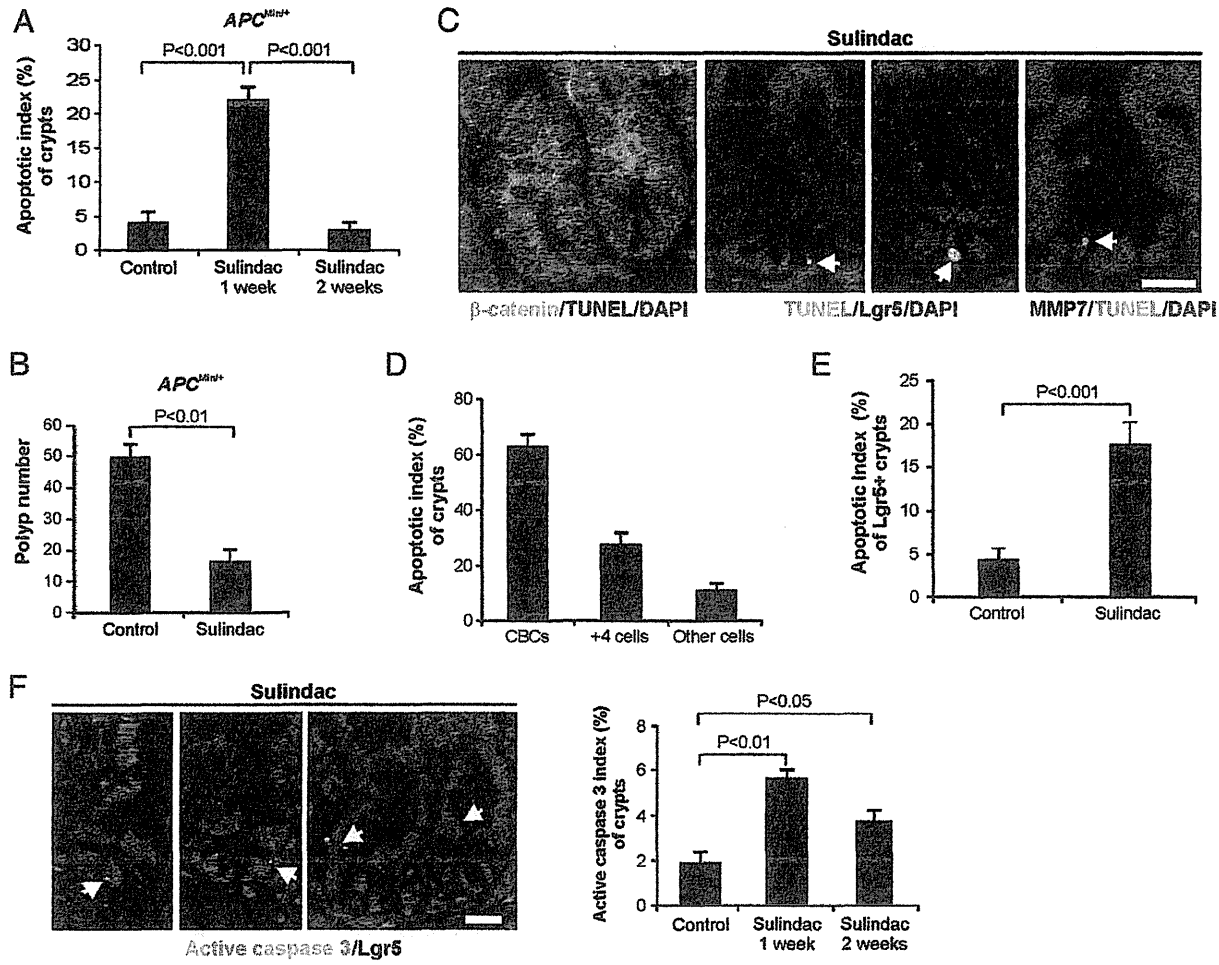

Fig. 1. Short-term sulindac administration induced apoptosis in the intestinal stem cells and suppressed adenoma formation in $APC^{Min/+}$ mice. Ten-week-old $APC^{Min/+}$ mice were fed with control or sulindac-containing (20 mg/kg/d) AIN93G diet for 1 or 2 wk and killed immediately after treatment. Intestinal polyp phenotypes, β-catenin localization, and apoptosis were analyzed. (*A*) Small intestinal sections from the treated mice were analyzed for apoptosis by TUNEL staining. The fractions of crypts containing at least one TUNEL-positive cell were determined. (*B*) Numbers of small intestinal polyps (≥0.5 mm in diameter) were counted following sulindac treatment for 1 wk. (*C*) Staining of indicated makers in $APC^{Min/+}$ mice treated with sulindac for 1 wk. For Lgr5 (EGFP) staining, $APC^{Min/+}$ mice containing the Lgr5-EGFP lineage marking allele (*Lgr5-EGFP/APC*$^{Min/+}$ mice) were analyzed. Lgr5 marks CBC cells and occasionally +4 cells, whereas MMP7 labels Paneth cells. DAPI (blue) was used for nuclear counter staining. Arrows indicate example TUNEL-positive CBCs (Lgr5-positive or MMP7-negative). (*D*) Quantification of TUNEL-positive cells based on locations in the crypts. Apoptotic index represents the fraction of crypts containing one or more TUNEL-positive cells. (*E*) Quantification of Lgr5-positive crypts containing one or more TUNEL-positive cells in *Lgr5-EGFP/APC*$^{Min/+}$ mice treated with control or sulindac diet for 1 wk. (*F*) *Left*: Staining of Lgr5 (red) and active caspase 3 (green) in $APC^{Min/+}$ mice treated with sulindac for 1 wk, with arrows indicating double positive cells. *Right*: Quantification of crypts containing one or more active caspase 3-positive cells. Values in *A*, *B*, and *D*–*F* are means ± SD (n = 6 in each group). At least 500 crypts from each animal were analyzed. (Scale bars: 15 μm.)

several neighboring Lgr5-positive crypts (Fig. 1 *C* and *F* and Fig. S3*A*), probably reflecting clonal expansion of the intestinal stem cells in which an early oncogenic event(s) occurred. These data demonstrate that intestinal stem cells are targeted for apoptosis induction following NSAID treatment.

Sulindac Treatment Removed Intestinal Stem Cells with β-Catenin Accumulation and Suppressed β-Catenin Phosphorylation. Intestinal polyp formation in $APC^{Min/+}$ mice is always accompanied by loss of the remaining WT *APC* allele (22), leading to deregulation of Wnt signaling and nuclear translocation of β-catenin (23). We therefore reasoned that sulindac may preferentially induce apoptosis in stem cells with nuclear β-catenin. Indeed, nuclear β-catenin was found in 1.92% of intestinal crypts in the control mice, including both the CBC and +4 cells, but rarely (<0.01% crypts) in other areas of the intestinal epithelium, or in the crypts of WT mice (Fig. 2*A*). Sulindac treatment for only 1 wk reduced the number of crypts containing cells with nuclear β-catenin by 75% (Fig. 2*A*). Interestingly, a vast majority (98%, 0.47%/0.48%) of identifiable CBC and +4 cells with nuclear β-catenin in sulindac-treated $APC^{Min/+}$ mice were TUNEL-positive at this time point (Fig. 2 *A* and *B*).

It has been shown that β-catenin nuclear translocation can be promoted by phosphorylation at Ser552 in the +4 cells (24). We found that the number of cells positive for β-catenin Ser552 phosphorylation (p-β-catenin), including mostly +4 and above +4 cells that did not express Lgr5 and some (11.4%) Lgr5-expressing cells (Fig. S5), was ninefold higher in $APC^{Min/+}$ mice compared with that in WT mice. Sulindac treatment significantly reduced cells with p-β-catenin (Fig. 2*C*), and induced rapid and significant apoptosis in these cells (Fig. 2*D*). These results suggest that sulindac treatment rapidly removes intestinal stem cells or progenitors with aberrant activation of Wnt signaling through induction of apoptosis.

NSAID Treatment Induced Apoptosis in Human Colonic Polyps and Removed Cells with Aberrant Wnt Signaling. To test the relevance of these observations in human patients, we analyzed colonic polyps

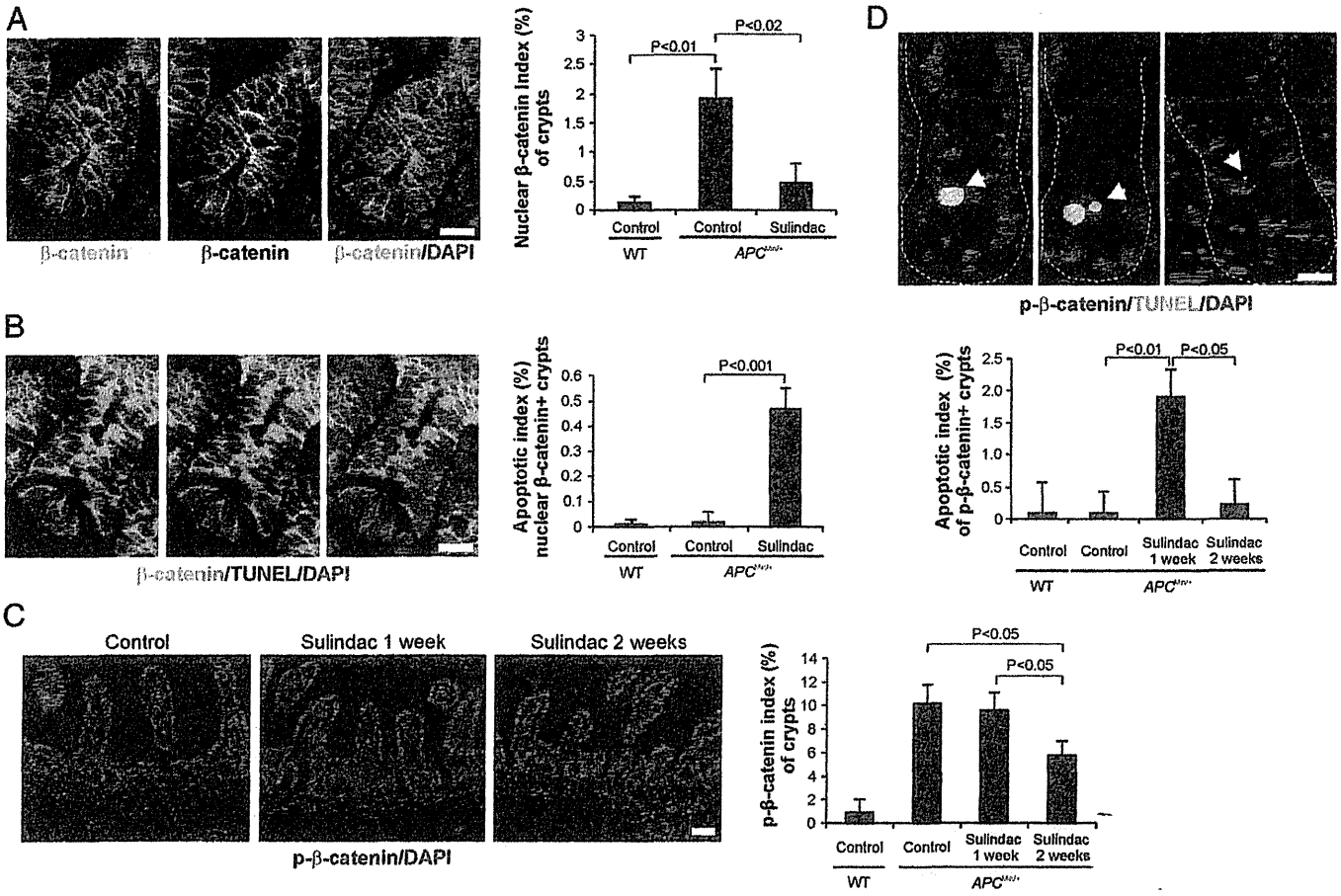

Fig. 2. Sulindac treatment removed the intestinal cells with nuclear or phospho-β-catenin via apoptosis. WT and $APC^{Min/+}$ mice were fed with control or sulindac-containing (20 mg/kg/d) diet for 1 or 2 wk and killed immediately after treatment. Small intestinal sections from the mice were analyzed for β-catenin localization, β-catenin Ser552 phosphorylation (p-β-catenin), and apoptosis (TUNEL) by immunostaining. (*A*) Analysis of β-catenin localization. *Left*: Staining of β-catenin (green or white) and DAPI (blue) in $APC^{Min/+}$ mice treated with sulindac for 1 wk. Circles mark representative CBCs with nuclear β-catenin. *Right*: Quantification of crypts with nuclear β-catenin in WT or $APC^{Min/+}$ mice treated with control or sulindac diet for 1 wk. (*B*) Analysis of β-catenin localization and apoptosis. *Left*: Staining of β-catenin (green), TUNEL (red), and DAPI (blue) in $APC^{Min/+}$ mice treated with sulindac for 1 wk. Circles mark example CBCs with nuclear β-catenin that were undergoing apoptosis. *Right*: Quantification of crypts positive for both nuclear β-catenin and TUNEL in WT and $APC^{Min/+}$ mice treated with control or sulindac diet for 1 wk. (*C*) Analysis of β-catenin phosphorylation. *Left*: Staining of p-β-catenin (red) and DAPI (blue) in $APC^{Min/+}$ mice treated with control or sulindac diet for 1 or 2 wk. *Right*: Quantification of crypts containing p-β-catenin-positive cells. (*D*) Analysis of β-catenin phosphorylation and apoptosis. *Upper*: Staining of p-β-catenin (red), TUNEL (green), and DAPI (blue) in $APC^{Min/+}$ mice treated with sulindac for 1 wk. Arrows indicate TUNEL and p-β-catenin double-positive cells. *Lower*: Quantification of crypts containing apoptotic cells in WT or $APC^{Min/+}$ mice treated with control or sulindac diet for 1 or 2 wk. Values in *A*–*D* are means ± SD ($n = 6$ in each group). At least 500 crypts from each animal were analyzed. (Scale bars: 15 μm.)

in patients taking NSAIDs. The percentage of colonic crypts containing TUNEL-positive apoptotic cells increased by more than 10-fold (from 5.04% to 51.9%) in the patients taking NSAIDs compared with those not taking NSAIDs (Fig. 3*A* and *B* and Fig. S6). TUNEL-positive cells could be detected among those stained positive for OLFM4, a Wnt target and a CBC cell marker (11, 25) (Fig. 3*C*). Interestingly, we found that the number of p-β-catenin-positive cells decreased drastically (by more than sixfold) in patients taking NSAIDs (Fig. 3*D*). These data suggest that NSAIDs selectively induce apoptosis in human intestinal polyps with aberrant Wnt signaling.

***SMAC* Deficiency Attenuated the Chemopreventive Effect of Sulindac.** Our previous work revealed that SMAC, a mitochondrial apoptogenic protein released into cytosol during apoptosis execution (15), is essential for NSAID-induced apoptosis in colon cancer cells (16, 17). To determine whether such a mechanism operates in vivo, age- and sex-matched cohorts of $APC^{Min/+}$ mice with WT *SMAC* ($APC^{Min/+}$) or *SMAC*-KO ($SMAC^{-/-}/APC^{Min/+}$) were generated and subjected to sulindac treatment for 1 wk. *SMAC* deficiency significantly attenuated the chemopreventive effect of sulindac in $APC^{Min/+}$ mice (50.2% vs. 69.6%; $P < 0.01$; Fig. 4*A* and Fig. S7*A*). A slight increase in polyp number in *SMAC*-deficient $APC^{Min/+}$ mice was observed, and taken into the consideration. Anatomic stratification revealed that the differences were mainly in the middle and distal regions, but not in the proximal region of small intestine (Fig. 4*B*). No significant difference in polyp size was found.

***SMAC* Deficiency Impaired Sulindac-Induced Apoptosis and Suppression of Nuclear β-Catenin Accumulation.** Following 1 wk of sulindac treatment, the number of crypts with TUNEL-positive CBC/+4 cells was significantly lower in the $SMAC^{-/-}/APC^{Min/+}$ mice than in $APC^{Min/+}$ mice (9.9% vs. 22.1%; $P < 0.005$; Fig. 4*C* and Fig. S7*B*). Apoptosis in the crypts decreased significantly in both strains following 2 wk of sulindac treatment (Fig. 4*C* and Fig. S7*C*). Similarly, the number of cells or crypts with nuclear β-catenin was significantly higher in $SMAC^{-/-}/APC^{Min/+}$ mice compared with that in $APC^{Min/+}$ mice (1.33% vs. 0.48%; $P < 0.05$; Fig. 4*D*), which was correlated with a significant decrease of apoptosis in the CBC/

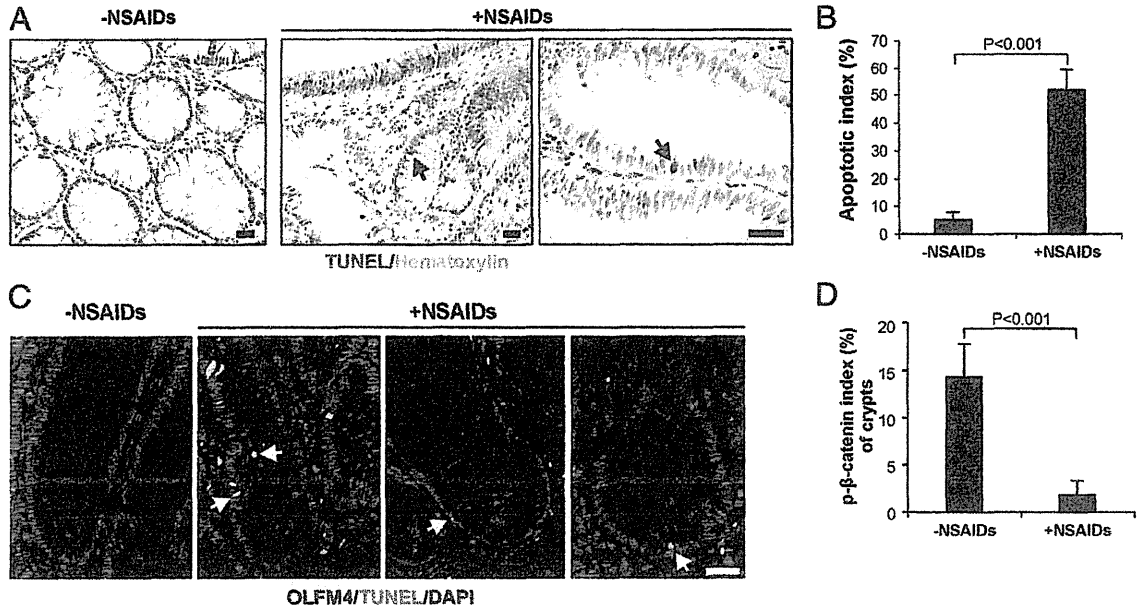

Fig. 3. NSAIDs induced apoptosis in human colonic polyps and removed cells with activated Wnt signaling. (*A*) TUNEL staining (brown) of intestinal polyps from patients taking or not taking NSAIDs. Arrows indicate TUNEL-positive apoptotic cells. (*B*) Quantification of crypts containing TUNEL-positive cells. Apoptotic index represents the percentage of intestinal crypts containing one or more TUNEL-positive cells. (C) Sections of intestinal polyps from four patients taking or not taking NSAIDs were stained for TUNEL (green), OLFM4 (red), and DAPI (blue). Arrows indicate TUNEL and OLFM4 double-positive cells. (*D*) Sections of intestinal polyps as in *C* were stained for p-β-catenin and quantified. Values in *B* and *D* are means ± SD ($n = 4$ in each group). At least 200 crypts from each patient were analyzed. (Scale bars: 15 μm.)

+4 cells with nuclear β-catenin (0.22% vs. 0.47%; $P < 0.05$; Fig. 4*E* and Fig. S7*B*). Furthermore, *SMAC* deficiency significantly impaired apoptosis and removal of p-β-catenin–positive cells in the crypts (Fig. 4 *F* and *G*). In addition, sulindac treatment did not affect SMAC expression in the mucosa of $APC^{Min/+}$ mice (Fig. S8*A*) and in colon cancer cells that undergo SMAC-dependent apoptosis (17) (Fig. S8*B*). These results demonstrate that SMAC-mediated apoptosis in the intestinal stem cells with aberrant activation of Wnt signaling directly contributes to chemoprevention.

Discussion

Neoplastic transformation appears to be driven by accumulation of genetic and epigenetic alterations in tissue stem cells or progenitors with pluripotency and regenerative potential (26, 27). Our results indicate that CBC and +4 intestinal stem cells accumulating nuclear or p-β-catenin are selectively removed by NSAIDs in $APC^{Min/+}$ mice through apoptosis induction, which translates into effective tumor prevention. Apoptosis in intestinal epithelial cells proceeds rapidly, typically within days (28), which may explain why we could detect sulindac-induced apoptosis only at an early time point. The partial effect of *SMAC* deficiency on sulindac-mediated chemoprevention is consistent with incomplete block of sulindac-induced apoptosis in *SMAC*-KO mice (Fig. 4*C*) and cells (17), and involvement of additional mechanisms including COX inhibition (29). The upstream events that activate Bax to trigger SMAC release following sulindac treatment remain to be delineated, and may involve death receptor signaling as suggested by several recent studies (30, 31).

Several characteristics of stem cells may explain the preferential killing of oncogenic stem cells by sulindac. Stem cells express high levels of "stemness" factors including the oncoprotein c-Myc (32), a well known apoptosis inducer (33). Therefore, stem cells with oncogenic alterations, such as loss of *APC*, may be more sensitive to NSAID-induced apoptosis, relative to differentiated cells with such alterations. It is also possible that stem cells with oncogenic alterations are simply more prevalent than differentiated cells with such alterations, because stem cells can regenerate and permanently keep acquired genetic changes, whereas differentiated cells with these changes may quickly disappear because of their rapid turnover.

Long-term use of NSAIDs, in particular COX2-specific inhibitors, is associated with side effects, which has stimulated active pursuit of new targets and combination strategies for cancer chemoprevention (34). Induction of apoptosis in oncogenic stem cells is likely to be a useful marker for successful cancer prevention, and may hold the promise for identifying novel and improved cancer chemopreventive agents. Small-molecule SMAC mimetics, which are in clinical development and can sensitize colon cancer cells to NSAID-induced apoptosis (16), may be useful as sensitizers of NSAIDs for safer and more effective cancer chemoprevention.

Methods

Mice and Treatment. All animal experiments were approved by the Institutional Animal Care and Use Committee at University of Pittsburgh. The *SMAC*-KO mice on a mixed background (129/C57BL/6) (35) were backcrossed to C57BL/6 background for 10 generations. Female $SMAC^{+/-}$ mice were crossed with $APC^{Min/+}$ mice (Jackson Laboratory) to generate $SMAC^{+/-}/APC^{Min/+}$ male mice, which were crossed to $SMAC^{+/-}$ mice to generate $APC^{Min/+}$ littermates with homozygous WT ($^{+/+}$) or null (i.e., KO; $^{-/-}$) *SMAC* alleles. The previously described *Lgr5-EGFP* (*Lgr5-EGFP*-IRES-creER^{T2}) mice (10) were crossed with $APC^{Min/+}$ mice to generate *Lgr5-EGFP*/$APC^{Min/+}$ mice. All mice were housed in micro isolator cages in a room illuminated from 7:00 AM to 7:00 PM (i.e., 12-h/12-h light-dark cycle), and allowed access to water and chow ad libitum. Genotyping was performed as previously described for *SMAC* (35) and for *Lgr5* (10). *APC* genotyping was according to the Jackson Laboratory protocol.

Treatment and Tumor Analysis. Ten-week-old and sex-matched $APC^{Min/+}$ mice with different *SMAC* and *Lgr5* genotypes were fed with control or experimental AIN93G diet (Dyets) containing 200 ppm (approximately 20 mg/kg/d) of sulindac (Sigma) for 1, 2, or 22 wk. Mice were killed immediately after treatment. Dissection of small intestine and histological analysis of adenomas (polyps; >0.5 mm in diameter) were performed as previously described (36). The adenoma counts were performed under a dissection microscope at various times following sulindac treatment.

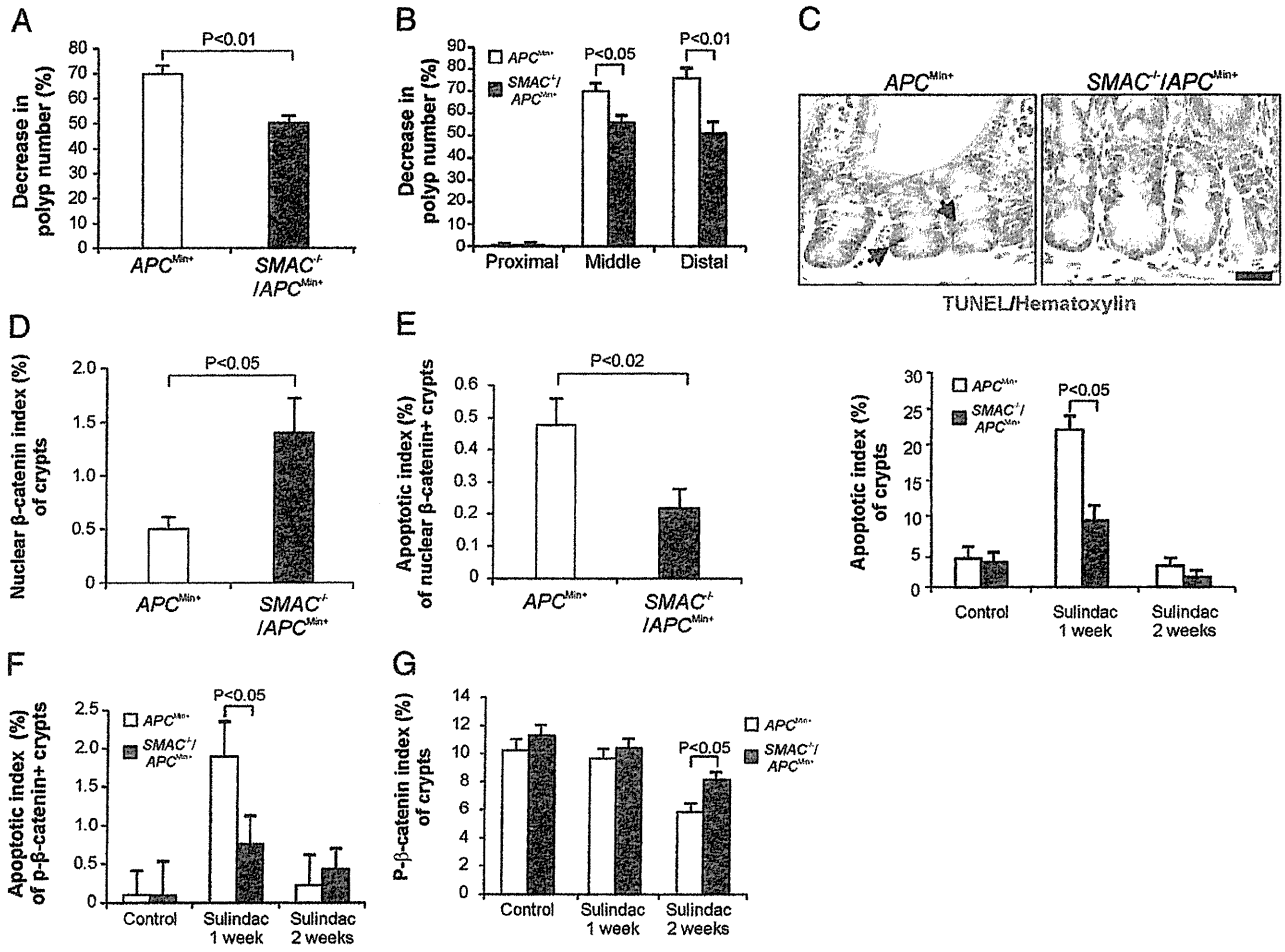

Fig. 4. *SMAC* deficiency attenuated the chemopreventive effect of sulindac in $APC^{Min/+}$ mice by blocking apoptosis in the intestinal stem cells. Age- and sex-matched parental ($APC^{Min/+}$) and *SMAC*-deficient $APC^{Min/+}$ mice ($SMAC^{-/-}/APC^{Min/+}$) were fed with control or sulindac-containing (20 mg/kg/d) diet for 1 or 2 wk and killed immediately after treatment. Intestinal polyp phenotypes, β-catenin localization, β-catenin Ser552 phosphorylation (p-β-catenin), and apoptosis were analyzed and compared. (*A*) Polyp (≥0.5 mm in diameter) number reduction in the treated mice. (*B*) Distribution of polyp number reduction in three different regions in the small intestine of the treated mice. (*C*) *Upper*: Staining of TUNEL (brown) and hematoxylin (blue) in the mice treated with sulindac for 1 wk. Arrows indicate example TUNEL-positive cells. (Scale bar: 15 μm.) *Lower*: Quantification of crypts containing one or more TUNEL-positive cells in the treated mice. (*D*) Fractions of crypts containing one or more CBC cells with nuclear β-catenin. (*E*) Fractions of crypts containing one or more TUNEL-positive cells with nuclear β-catenin. (*F*) Fractions of crypts containing one or more p-β-catenin and TUNEL double-positive cells. (*G*) Fractions of crypts containing one or more p-β-catenin–positive cells. Values are means ± SD; $n = 6$ in each group in *A–D*; $n = 4$ in each group in *E–G*. At least 500 crypts from each animal were analyzed.

Immunostaining. Tissue sections (5 μm) were deparaffinized, rehydrated, and treated with 3% hydrogen peroxide, followed by antigen retrieval in boiling 0.1 M citrate (pH 6.0) buffer for 10 min twice. The sections were then blocked by 20% goat/rabbit serum for 30 min. TUNEL staining was performed by using an ApopTag Kit (Chemicon International) according to the manufacturer's protocol. Immunostaining was performed as previously described for MMP7 (21), active caspase 3 (37), and OLFM4 (25). EGFP staining was performed at 4 °C overnight using a mouse anti-EGFP antibody (Santa Cruz Biotechnology), with Alexa 594 (Invitrogen) for signal detection. β-Catenin staining was done at 4 °C overnight using a mouse anti-β-catenin antibody (BD Biosciences), with Alexa 488 (Invitrogen) for signal detection. Staining of p-β-catenin Ser552 was performed as described (24). For double staining, TUNEL staining was performed following EGFP, β-catenin, p-β-catenin, OLFM4, or MMP-7 staining. EGFP staining was performed before MMP7, p-β-catenin, or active caspase 3 staining. Cells with positive staining were scored in at least 500 crypt sections and reported as mean ± SD.

Clinical Samples. Frozen specimens of polyps from four patients taking NSAIDs and four patients not taking NSAIDs were obtained from the Digestive Disease Tissue Resource of the University of Pittsburgh. Acquisition of tissue samples was approved by the institutional review board at the University of Pittsburgh and written informed consent was received from each patient. Paraffin blocks and sections were prepared as previously described (21) and analyzed by immunostaining.

Two male and two female subjects were represented in each category, with ages ranging from 50 to 65 y in the NSAID group and 58 to 75 y in the non-NSAID group. Subjects taking NSAIDs reported use ranging from one to three tablets per week to greater than seven tablets per week during the preceding year. The specific NSAIDs in use were not recorded. All patients had advanced adenomas by virtue of having polyps at least 1 cm in size. Four patients had tubulovillous histology and four had tubular adenomas.

Statistical Analysis. Statistical analyses were carried out using GraphPad Prism IV software. *P* values were calculated by the Student's *t* test. $P < 0.05$ was considered to be significant. The means ± 1 SD are displayed in the figures where applicable.

ACKNOWLEDGMENTS. We thank Dr. Monica E. Buchanan and other members of the L.Z. and J.Y. laboratories for helpful discussion and advice, Dr. Ronald A. DePinho at the Dana-Farber Cancer Institute (Boston, MA) for providing rederived *Lgr5-EGFP* mice, and Dr. Linheng Li at the Stowers Institute for Medical Research (Kansas City, MO) for providing the phospho-β-catenin antibody. This work was supported in part by National Institutes of Health Grants CA121105 (to L.Z.), CA106348 (to L.Z.), CA129829 (to J.Y.), and U01-DK085570 (to J.Y.), the latter as part of the Intestinal Stem Cell Consortium, a collaborative research project funded by the National Institute of Diabetes and Digestive and Kidney Diseases. This work was also supported by American Cancer Society Grants RSG-07-156-01-CNE (to L.Z.) and RGS-10-124-01-CCE (to J.Y.) and a grant from the Flight Attendant Medical Research Institute (to J.Y.).

1. Hong WK, Sporn MB (1997) Recent advances in chemoprevention of cancer. *Science* 278:1073–1077.
2. Stoner GD (2009) Foodstuffs for preventing cancer: The preclinical and clinical development of berries. *Cancer Prev Res (Phila)* 2:187–194.
3. Thun MJ, Henley SJ, Patrono C (2002) Nonsteroidal anti-inflammatory drugs as anticancer agents: Mechanistic, pharmacologic, and clinical issues. *J Natl Cancer Inst* 94:252–266.
4. Rao CV, Reddy BS (2004) NSAIDs and chemoprevention. *Curr Cancer Drug Targets* 4: 29–42.
5. Vogelstein B, Kinzler KW (2004) Cancer genes and the pathways they control. *Nat Med* 10:789–799.
6. Su LK, et al. (1992) Multiple intestinal neoplasia caused by a mutation in the murine homolog of the APC gene. *Science* 256:668–670.
7. Barker N, et al. (2009) Crypt stem cells as the cells-of-origin of intestinal cancer. *Nature* 457:608–611.
8. Sangiorgi E, Capecchi MR (2008) Bmi1 is expressed in vivo in intestinal stem cells. *Nat Genet* 40:915–920.
9. Li L, Clevers H (2010) Coexistence of quiescent and active adult stem cells in mammals. *Science* 327:542–545.
10. Barker N, et al. (2007) Identification of stem cells in small intestine and colon by marker gene Lgr5. *Nature* 449:1003–1007.
11. van der Flier LG, Haegebarth A, Stange DE, van de Wetering M, Clevers H (2009) OLFM4 is a robust marker for stem cells in human intestine and marks a subset of colorectal cancer cells. *Gastroenterology* 137:15–17.
12. Yu J, Zhang L (2004) Apoptosis in human cancer cells. *Curr Opin Oncol* 16:19–24.
13. Sun SY, Hail N, Jr., Lotan R (2004) Apoptosis as a novel target for cancer chemoprevention. *J Natl Cancer Inst* 96:662–672.
14. Zhang L, Yu J, Park BH, Kinzler KW, Vogelstein B (2000) Role of BAX in the apoptotic response to anticancer agents. *Science* 290:989–992.
15. Du C, Fang M, Li Y, Li L, Wang X (2000) Smac, a mitochondrial protein that promotes cytochrome c-dependent caspase activation by eliminating IAP inhibition. *Cell* 102: 33–42.
16. Bank A, Wang P, Du C, Yu J, Zhang L (2008) SMAC mimetics sensitize nonsteroidal anti-inflammatory drug-induced apoptosis by promoting caspase-3-mediated cytochrome c release. *Cancer Res* 68:276–284.
17. Kohli M, et al. (2004) SMAC/Diablo-dependent apoptosis induced by nonsteroidal antiinflammatory drugs (NSAIDs) in colon cancer cells. *Proc Natl Acad Sci USA* 101: 16897–16902.
18. Beazer-Barclay Y, et al. (1996) Sulindac suppresses tumorigenesis in the Min mouse. *Carcinogenesis* 17:1757–1760.
19. McEntee MF, Chiu CH, Whelan J (1999) Relationship of beta-catenin and Bcl-2 expression to sulindac-induced regression of intestinal tumors in Min mice. *Carcinogenesis* 20:635–640.
20. Corpet DE, Pierre F (2003) Point: From animal models to prevention of colon cancer. Systematic review of chemoprevention in min mice and choice of the model system. *Cancer Epidemiol Biomarkers Prev* 12:391–400.
21. Qiu W, et al. (2008) PUMA regulates intestinal progenitor cell radiosensitivity and gastrointestinal syndrome. *Cell Stem Cell* 2:576–583.
22. Shoemaker AR, Gould KA, Luongo C, Moser AR, Dove WF (1997) Studies of neoplasia in the Min mouse. *Biochim Biophys Acta* 1332:F25–F48.
23. Clevers H (2006) Wnt/beta-catenin signaling in development and disease. *Cell* 127: 469–480.
24. He XC, et al. (2007) PTEN-deficient intestinal stem cells initiate intestinal polyposis. *Nat Genet* 39:189–198.
25. Oue N, et al. (2009) Serum olfactomedin 4 (GW112, hGC-1) in combination with Reg IV is a highly sensitive biomarker for gastric cancer patients. *Int J Cancer* 125: 2383–2392.
26. Rosen JM, Jordan CT (2009) The increasing complexity of the cancer stem cell paradigm. *Science* 324:1670–1673.
27. Yu J (2009) PUMA kills stem cells to stall cancer? *Mol Cell Pharmacol (Windsor Mill)* 1: 112–118.
28. Hall PA, Coates PJ, Ansari B, Hopwood D (1994) Regulation of cell number in the mammalian gastrointestinal tract: The importance of apoptosis. *J Cell Sci* 107: 3569–3577.
29. Keller JJ, Giardiello FM (2003) Chemoprevention strategies using NSAIDs and COX-2 inhibitors. *Cancer Biol Ther* 2(suppl 1):S140–S149.
30. Deng Y, Ren X, Yang L, Lin Y, Wu X (2003) A JNK-dependent pathway is required for TNFalpha-induced apoptosis. *Cell* 115:61–70.
31. Zhang L, et al. (2010) Chemoprevention of colorectal cancer by targeting APC-deficient cells for apoptosis. *Nature* 464:1058–1061.
32. Yu J, et al. (2007) Induced pluripotent stem cell lines derived from human somatic cells. *Science* 318:1917–1920.
33. Hermeking H, Eick D (1994) Mediation of c-Myc-induced apoptosis by p53. *Science* 265:2091–2093.
34. Meyskens FL, Jr., et al. (2008) Difluoromethylornithine plus sulindac for the prevention of sporadic colorectal adenomas: A randomized placebo-controlled, double-blind trial. *Cancer Prev Res (Phila)* 1:32–38.
35. Okada H, et al. (2002) Generation and characterization of Smac/DIABLO-deficient mice. *Mol Cell Biol* 22:3509–3517.
36. Qiu W, Carson-Walter EB, Kuan SF, Zhang L, Yu J (2009) PUMA suppresses intestinal tumorigenesis in mice. *Cancer Res* 69:4999–5006.
37. Qiu W, Leibowitz B, Zhang L, Yu J (2010) Growth factors protect intestinal stem cells from radiation-induced apoptosis by suppressing PUMA through the PI3K/AKT/p53 axis. *Oncogene* 29:1622–1632.

Published OnlineFirst August 10, 2010; DOI:10.1158/0008-5472.CAN-09-4701

Cancer Research

CDX2 Regulates *Multidrug Resistance 1* Gene Expression in Malignant Intestinal Epithelium

Yuji Takakura, Takao Hinoi, Naohide Oue, et al.

Cancer Res 2010;70:6767-6778. Published OnlineFirst August 10, 2010.

Published OnlineFirst August 10, 2010; DOI:10.1158/0008-5472.CAN-09-4701

Cancer Research

CDX2 Regulates *Multidrug Resistance 1* Gene Expression in Malignant Intestinal Epithelium

Yuji Takakura[1], Takao Hinoi[2], Naohide Oue[3], Tatsunari Sasada[1], Yasuo Kawaguchi[1], Masazumi Okajima[2], Aytekin Akyol[4], Eric R. Fearon[4], Wataru Yasui[3], and Hideki Ohdan[1]

Abstract

The caudal-related homeobox transcription factor CDX2 has a key role in intestinal development and differentiation. *CDX2* heterozygous mutant mice develop colonic polyps, and loss of CDX2 expression is seen in a subset of colon carcinomas in humans. Ectopic CDX2 expression in the stomach of transgenic mice promotes intestinal metaplasia, and CDX2 expression is frequently detected in intestinal metaplasia in the stomach and esophagus. We sought to define CDX2-regulated genes to enhance knowledge of CDX2 function. HT-29 colorectal cancer cells have minimal endogenous CDX2 expression, and HT-29 cells with ectopic CDX2 expression were generated. Microarray-based gene expression studies revealed that the *Multidrug Resistance 1* (*MDR1/P-glycoprotein/ABCB1*) gene was activated by CDX2. Evidence that the *MDR1* gene was a direct transcriptional target of CDX2 was obtained, including analyses with *MDR1* reporter gene constructs and chromatin immunoprecipitation assays. RNA interference–mediated inhibition of CDX2 decreased endogenous *MDR1* expression. In various colorectal cancer cell lines and human tissues, endogenous *MDR1* expression was well correlated to CDX2 expression. Overexpression of CDX2 in HT-29 cells revealed increased resistance to the known substrate of *MDR1*, vincristine and paclitaxel, which was reversed by an *MDR1* inhibitor, verapamil. These data indicate that CDX2 directly regulates *MDR1* gene expression through binding to elements in the promoter region. Thus, CDX2 is probably important for basal expression of *MDR1*, regulating drug excretion and absorption in the lower gastrointestinal tract, as well as for multidrug resistance to chemotherapy reagent in CDX2-positive gastrointestinal cancers. *Cancer Res; 70(17); 6767–78. ©2010 AACR.*

Introduction

There has long been great interest in defining critical regulatory factors that direct cell fate determination and differentiation in normal and cancer tissues. In mammals, the CDX1 and CDX2 homeobox transcription factors apparently have critical functions in intestinal development, differentiation, and maintenance of the intestinal phenotype (1, 2). CDX1 and CDX2 proteins show significant homology, particularly in their homeobox DNA–binding domains, to the protein product of the *Drosophila caudal gene*, a key regulator of anterior-posterior regional identity (1, 3, 4). Mouse *Cdx1* and *Cdx2* genes are quite broadly expressed during early embryonic development. Recent studies indicated that Cdx2 is one of the earliest transcription factors essential for formation and maintenance of the trophectoderm lineage in mouse embryos (5, 6). However, in later stages of development and in normal adult tissues, expression of the genes is apparently restricted to epithelium of the small intestine and colon (1). In support of the view that CDX proteins play key roles in regulating proliferation and intestinal cell fate, mice with constitutional inactivating mutations in one *Cdx2* allele (*Cdx2±*) developed multiple polyps in the proximal colon (7–10). The epithelial cells in these polyps often lose intestinal differentiation features, displaying areas of stratified squamous epithelium similar to that in forestomach and distal esophagus as well as areas resembling normal gastric mucosa (7, 11). Ectopic expression of *Cdx2* in the gastric mucosa of transgenic mice was reported to induce intestinal metaplasia (12, 13). In humans, loss of the *CDX1* and/or *CDX2* gene and protein expression was observed in a subset of primary colorectal cancers (CRC) and cancer cell lines (14), usually in poorly differentiated CRCs (15). Aberrant (ectopic) expression of CDX2 is detected frequently in intestinal metaplasia of the stomach (16, 17).

Our prior efforts to identify CDX2-regulated genes indicated that liver intestine-cadherin (LI-cadherin) and hephaestin

Authors' Affiliations: Departments of [1]Surgery, [2]Endoscopic Surgery and Surgical Science, and [3]Molecular Pathology, Division of Frontier Medical Science, Programs for Biomedical Research, Graduate School of Biomedical Science, Hiroshima University, Hiroshima, Japan; and [4]Division of Molecular Medicine and Genetics, Departments of Internal Medicine, Human Genetics, and Pathology, University of Michigan Medical School, Ann Arbor, Michigan

Note: Supplementary data for this article are available at Cancer Research Online (http://cancerres.aacrjournals.org/).

Present address for A. Akyol: Hacettepe University School of Medicine, Department of Pathology, Ankara, Turkey.

Corresponding Author: Takao Hinoi, Department of Endoscopic Surgery and Surgical Science, Hiroshima Universtiy, 1-2-3 Kasumi, Minami-ku, Hiroshima, 734-8551, Japan. Phone: 81-82-257-5222; Fax: 81-82-257-5224; E-mail: thinoi@hiroshima-u.ac.jp.

doi: 10.1158/0008-5472.CAN-09-4701

Published OnlineFirst August 10, 2010; DOI:10.1158/0008-5472.CAN-09-4701

(HEPH) were likely key molecules regulated by CDX2 in normal and malignant gastrointestinal epithelium (16, 18).

Here, we report on further studies to implicate CDX2 in regulating the expression of intestinal-specific genes by using high-density oligonucleotide microarrays as a starting point to identify potential CDX2-regulated genes in HT-29, a CRC cell line with significantly decreased endogenous CDX2 expression. In HT-29 cell line engineered to express CDX2 ectopically, the gene for *Multidrug Resistance 1* (*MDR1*) was strongly activated.

Of some potential interest, *MDR1* was originally identified as an overexpressed and amplified gene in multiple drug-resistant cells, and its product, P-glycoprotein, seems to play a critical role in drug resistance (19). We provide data here implicating CDX2 as an important factor in regulation of *MDR1* expression in gastrointestinal tissues.

Materials and Methods

Plasmids

A full-length, wild-type *CDX2* and *CDX1* allele were amplified by PCR using hexamer-primed complementary DNA (cDNA) from normal human colon tissue as a template. Sequence coding Flag epitope was added to the 5′ ends of *CDX1* allele. The *CDX2* and Flag-*CDX1* allele were inserted into the multiple cloning site of the retroviral expression vector pPGS-CMV-CITE-neo (pPGS-neo, provided by G. Nabal, NIH, Bethesda, MD) to generate pPGS-CDX2. The full-length, wild-type *CDX2* allele was also subcloned into the retroviral vector pBabe-Puro ER (provided by A. Friedman, Johns Hopkins Oncology Center, Baltimore, MD; ref. 20) to generate pCDX2-ER. The pCDX2-ER vector encodes a chimeric protein in which full-length CDX2 sequences are fused upstream of a mutated estrogen receptor (ER) ligand–binding domain. The mutated ER ligand–binding domain no longer binds estrogen, but retains the ability to bind tamoxifen. Fragments from human *MDR1* and *glyceraldehyde-3-phosphate dehydrogenase* (*GAPDH*) genes were generated by PCR using hexamer-primed cDNA from Caco2 cells as a template (16). A 309-bp fragment of *MDR1* cDNA was amplified using forward primer 5′-CAGTGAACTCTGACTCTATGAGATG-3′ and reverse primer 5′-AGCAAGGCAGTCAGTTACAGTCC-3′. The *MDR1* and *GAPDH* cDNA fragments were subcloned into the pGEM-T Easy Vector (Promega). Genomic DNA sequences from the promoter regions of the human *MDR1* gene were cloned by PCR, using genomic DNA purified from DLD-1 cells as a template, with the reverse primer 5′-GGCTCGAG-GAAACAGGTTGAATTTCCAGG-3′ and the following forward primers: 5′-GCGGGTACCAGGCATTTAGCCTACTAGTG-3′ (from −4,003), 5′-ATGGTACCACATGTGAAAGG-GTGGAGAGTG-3′ (from −3,414), 5′-CCGGTACC-ATGTCAGTGGAGCAAAGAAATG-3′ (from −1,711), and 5′-CCGGTACCGTGAACAATGCTGTACACTTGC-3′ (from −1,422). The PCR products were digested with KpnI and XhoI (sites underlined in the primers) and subcloned into pGL4.10 [*luc2*] vector (Promega). PCR-based approaches were used to introduce mutations into the presumptive CDX2-binding sites in the pGL4.10-MDR1 (−4,203/+50) reporter gene construct. Sequence of presumptive CDX2 binding site A (ATTTATG) and B (TTTTATG) were changed to ACCTGCG and TCCTGCG in the primer using the primers: 5′-GCGGTACCAGGCATTTAGCCTACTAGTGTAATTTCC-GCAGGTC-3′ and 5′-GAGCGGGCTTCTCAGATGA-TATGTGCTTTTCACTCTGTGC-3′ (for binding site A), and 5′-GCGGGTACCAGGCATTTAGCCTACTAGTG-3′, 5′-GCATGTCCTTCATACGCAGGAATCATTACATGTG-3′, 5′-GCGTATGAAGGACATGTGATGATAGGGG-3′, and 5′-GGGCTTCTCAGATGATATGTGCTTTTCACTC-3′ (for binding site B). All fragments generated by PCR were verified by automated sequencing of the respective plasmid constructs. Plasmid pGL4.74 [*hRluc*/TK] vector (Promega) was used as control for transfection efficiency in reporter assays.

Cell culture and retrovirus infections

The amphotropic Phoenix packaging cell line was provided by G. Nolan (Stanford University, Stanford, CA). All other cell lines were obtained from the American Type Culture Collection in 1998 to 2000. Frozen stock was made immediately and stored in liquid nitrogen until the initiation of this study. After thawing frozen stock, the cells were kept at low passage throughout the study. The cell morphology was monitored by microscopy and confirmed that their morphologic images were maintained in comparison with the original morphologic images. Details of cell culture conditions were previously described (16). The Phoenix packaging cells were transfected with retroviral expression constructs (pPGS-CDX2, pPGS-neo, pPGS-Flag-CDX1, and pCDX2-ER); the supernatant containing nonreplicating amphotropic virus was harvested as previously described (16). HT-29 cells were infected with virus, selected, and maintained in media containing G418 (Invitrogen) or Puromycin (Sigma). In HT-29 cells expressing the CDX2-ER fusion protein (HT-29/CDX2-ER), CDX2 function was activated by addition of 4-hydroxytamoxifen (4-OHT; Sigma) to the growth medium at a final concentration of 500 nmol/L. To assess *MDR1* as a direct CDX2-regulated target gene, HT-29/CDX2-ER cells were treated with the protein synthesis inhibitor cycloheximide (Sigma) at a concentration of 1 μg/mL.

Complementary RNA synthesis and gene expression profiling

Total RNA was prepared by Trizol (Invitrogen) extraction and purification with the RNeasy Cleanup kit (Qiagen). Gene expression analyses were performed with GeneChip Human Genome U95Av2 and U133A (Affymetrix, Inc.) following supplier instructions. Affymetrix arrays were scanned using the GeneArray scanner (Affymetrix); image analysis was performed with the GeneChip 4.0 software (Affymetrix).

Northern blot analysis

For each sample, 10 μg of total RNA were fractionated by electrophoresis and transferred to a Zeta-Probe GT membrane (Bio-Rad Laboratories). Hybridization was performed using ^{32}P-radiolabeled cloned cDNA fragments of *MDR1*, as previously described (16). The membrane was stripped and reprobed with *GAPDH* cDNA to confirm equivalent loading and RNA transfer.

Published OnlineFirst August 10, 2010; DOI:10.1158/0008-5472.CAN-09-4701

Western blot assays

Western blot analysis was performed essentially as previously described (16). Anti-CDX2 mouse monoclonal antibodies (clone 7C7/D4, BioGenex Laboratories, Inc.), antihuman MDR1 monoclonal antibody (clone C219, Calbiochem), and anti-Flag M2 monoclonal antibody (Sigma) were used at 1:10,000, 1:50, and 1:500 dilutions, respectively. The membrane was stripped and reprobed with an anti–β-actin monoclonal antibody (clone AC-15; Sigma) to verify loading and transfer.

RNA interference

Two small interfering RNA (siRNA) duplexes targeting CDX2 (5′-AACCAGGACGAAAGACAAAUA-3′, CDX2 siRNA-1; and 5′-AAGCCUCAGUGUCUGGCUCUG-3′, CDX2 siRNA-2) and a nonsilencing siRNA duplex (5′-AAUUCUCCGAACGUGUCACGU-3′) were synthesized by Qiagen-Xeragon. Cells were cultured in antibiotic-free medium for 24 hours before transfection. They were then transfected with siRNA (340 pmol) using DharmaFECT1 (Dharmacon). Silencing was examined 72 hours after transfection. Each sample was reverse transcribed using the ReverTra Ace qPCR RT kit (Toyobo) following supplier protocols. Quantitative PCR (qPCR) analysis was performed on an ABI 7500HT with Power SYBR Green PCR Master Mix (Applied Biosystems). *MDR1* primers were as follows: forward, 5′-ATAATGCGACAGGAGATAGG-3′; and reverse, 5′-CCAAAATCACAAGGGTTAGC-3′. GAPDH primers were as follows: forward, 5′-TTGAGGTCAATGAAGGGG-3′; and reverse, 5′-GAAGGTGAAGGTCGGAGTC-3′. All experiments were conducted three times. Human GAPDH was measured as the internal control.

Reporter gene assays

At 48 hours before transfection, cells were seeded in 35-mm dishes. HT29/PGS-CDX2 and HT29/PGS-neo cells were transfected at 50% to 80% confluency with 4 μL of Lipofectamine 2000 (Invitrogen), 0.5 μg of pGL4.10 reporter gene construct, and 0.05 μg of control plasmid pGL4.74. At 40 hours after transfection, cells were collected and resuspended in passive lysis buffer (Promega). Luciferase activity was determined with a dual luciferase assay system (GloMax96 Microplate Luminometer, Promega).

Chromatin immunoprecipitation assay

The chromatin immunoprecipitation (ChIP) assays were performed using the ChIP-IT Express kit (Active Motif) following supplier instructions. Chromatin extracts containing DNA fragments (average size, 500 bp) were immunoprecipitated using 2 μg monoclonal anti-*CDX2* antibody (7C7/D4) or 2 μg nonimmunized mouse IgG whole molecule (negative control, Active Motif). Fragments (200 bp) of the *MDR1* promoter regions were PCR amplified using the primers 5′-CCTGGGAGACAGAGTAATAC-3′ (forward) and 5′-CAAACTGGACAGAGACTTATAC-3′ (reverse; −4,100/−3,882, including binding site A), and 5′-ATCCCCTATCAAGTACAGTC-3′ (forward) and 5′-CTCAGTCCAAAGAGCAAGAC-3′ (reverse; −3,482/−3,296, including binding site B). As a negative control, a .4-kb DNA fragment from exon 3 of the *CDX1* gene was amplified by PCR using previously described primers (18). Each immunoprecipitated DNA sample was quantified using the average of duplicate qPCRs. All ChIP-qPCR signals were normalized to the input (labeled as IP/input). Each primer gave a single product of the right size, as confirmed by agarose gel electrophoresis.

Immunohistochemical staining

Formalin-fixed, paraffin-embedded tissues were stained using the avidin-biotin complex method as previously described (16). Mouse monoclonal anti-CDX2 antibody 7C7/D4 and mouse monoclonal anti-MDR1 antibody (clone C494; Zymed Laboratories) were used at 1:1,000 and 1:10 dilution, respectively.

Cytotoxicity assay

Paclitaxel and verapamil were purchased from Sigma, and 5-fluorouracil was provided by Kyowa Hakko Kogyo Co. Ltd. Doxorubicin and vincristine were provided by Nippon Kayaku. Camptothecin and cisplatin were purchased from LKT Laboratories. MTT cytotoxicity assay was used to examine cell survival after exposure to chemotherapeutic agents. Cells were seeded at 5,000 cells/100 μL per well in 96-well microtiter plates. After a 48-hour incubation period, cells were treated with a range of concentrations of each chemotherapeutic agent. To examine the effect of verapamil, a known P-glycoprotein inhibitor (21), 2 μmol/L were administered together with each chemotherapeutic agent. A pilot experiment showed that this concentration was not cytotoxic to HT-29/PGS-CDX2 or HT-29/PGS-neo cells (data not shown). After 72 hours, 10 μL of MTT dye (5 mg/mL) was added to each well, and plates were incubated for 4 hours at 37°C in a humidified 5% CO_2 atmosphere. Dark blue formazan crystals formed by live cells were dissolved in 100 μL of solubilization solution (10% SDS in 0.01 mol/L HCl). Absorbance in individual wells was determined at 570 nm using an MTP-300 microplate reader (CORONA Electric Co. Ltd.). Results were expressed in terms of the concentration required to inhibit cell growth by 50% relative to nontreated cells [IC_{50} (72 h)].

Results

CDX2 and *MDR1* expression are correlated in colon carcinoma cells

Similar to a few selected other human CRC cell lines, the HT-29 line shows very low endogenous CDX2 expression (22). To identify candidate CDX2-regulated genes, we generated polyclonal populations of HT-29 CRC cells ectopically expressing CDX2, by infecting the cells with replication-defective retroviruses carrying full-length human *CDX2* cDNA (Fig. 1A). Comparison of gene expression in the HT-29/PGS-CDX2 cells versus control populations (HT-29/PGS-neo) was performed using microarrays with focus on the *MDR1* (*ABCB1*) gene. Affymetrix data indicated that *MDR1* gene expression was upregulated by CDX2 by roughly 31.14-fold in HT-29 cells (Fig. 1A). Northern and Western blot studies confirmed robust induction of *MDR1* transcripts and protein in HT-29/PGS-CDX2 cells (Fig. 1B). To determine whether MDR1 is a selective CDX2 target, we also generated polyclonal

Published OnlineFirst August 10, 2010; DOI:10.1158/0008-5472.CAN-09-4701

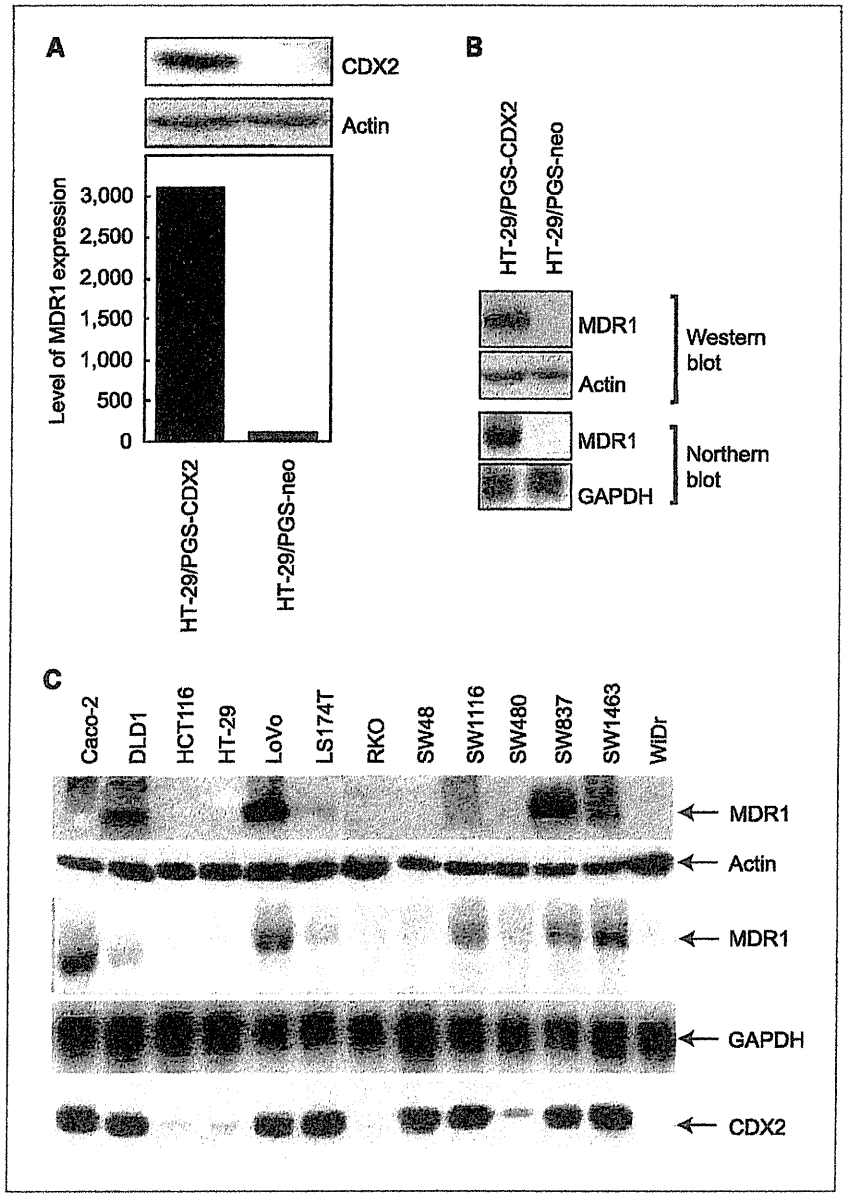

Figure 1. CDX2 activates *MDR1* expression in HT-29 cells. A, top, a monoclonal anti-CDX2 antibody detects the roughly 40-kDa CDX2 protein in HT-29/PGS-CDX2 cells but not in HT-29/PGS-neo cells. A, bottom, relative level of *MDR1* gene expression in HT-29/PGS-CDX2 and HT-29/PGS-neo in Affymetrix microarray studies. B, Northern and Western blot analysis detects *MDR1* transcripts and products in HT-29/PGS-CDX2 with low or absent *MDR1* expression in HT-29/PGS-neo cells. In Western blot analysis, a mouse monoclonal anti-MDR1 antibody detects the roughly 170-kDa *MDR1* product in HT-29/PGS-CDX2 cells but not in HT-29/PGS-neo cells. C, expression of CDX2 and *MDR1* in 13 CRC cell lines. In the indicated 13 CRC cell lines, Western blot analyses of MDR1 and CDX2 expression were performed using a mouse monoclonal antibody against human MDR1 and a mouse monoclonal antibody against human CDX2. The membranes were stripped and reprobed with a monoclonal antibody against β-actin to verify loading and transfer. Northern blot analysis of *MDR1* expression was performed using an *MDR1* cDNA probe. The membrane was stripped and reprobed with a GAPDH cDNA probe to verify loading and transfer.

populations of HT-29 cells ectopically expressing CDX1 (HT-29/PGS-Flag-CDX1). In this cell line, MDR1 expression was not induced by overexpression of CDX1 (Supplementary Fig. S1).

To assess the correlation between endogenous *CDX2* and *MDR1* expression in other CRC cell lines, Northern and Western blot analyses were performed on 12 additional lines. MDR1 protein expression was detected in six cell lines with high levels of *MDR1* transcripts. In all of these cell lines, strong CDX2 expression was observed (Fig. 1C, lanes 1, 2, 5, 9, 11, and 12, 5, 9, 11, and 12). However, none of the cell lines with weak or undetectable CDX2 expression had detectable *MDR1* transcripts or protein.

The *MDR1* gene is a primary target of CDX2 activity

To better assess the relationship between CDX2 function and *MDR1* gene expression, we studied *MDR1* expression in an HT-29–derived line with tightly regulated CDX2 activity. We used a polyclonal HT-29 cell line that had been transduced with a vector encoding a chimeric CDX2-ER fusion protein. In the chimeric CDX2-ER protein, full-length CDX2 sequences are present upstream of a mutated ER ligand–binding domain. The mutant ER ligand–binding domain is capable of binding to 4-OHT, but not estrogen. Expression of the CDX2-ER fusion protein in HT-29/CDX2-ER polyclonal cell line was confirmed (data not shown). Treatment of HT-29/CDX2-ER cell line with 4-OHT strongly induced *MDR1* expression within 12 hours, with further increased expression up to day 2 of 4-OHT treatment (Fig. 2A). Consistent with the notion that *MDR1* is a direct or primary target gene regulated by CDX2, blockade of new protein synthesis by cycloheximide treatment did not inhibit induction of *MDR1*

Published OnlineFirst August 10, 2010; DOI:10.1158/0008-5472.CAN-09-4701

transcripts at the 12-hour time point (Fig. 2B). However, as expected, cycloheximide treatment blocked induction of *MDR1* protein expression in 4-OHT–treated HT-29/CDX2-ER cells (Fig. 2B).

Inhibition of CDX2 by RNA interference results in the downregulation of *MDR1* in colon cancer cells

To determine whether CDX2 is necessary for *MDR1* expression in mammalian cells, we analyzed the effect of inhibiting CDX2 expression by RNA interference in the level of *MDR1* expression. DLD-1, a CRC cell line with high endogenous CDX2 and *MDR1* expression, was used. CDX2-specific siRNAs significantly suppressed CDX2 protein expression 3 days after transfection, and expression of *MDR1* transcript was downregulated roughly 50% by CDX2 siRNAs in DLD1 compared with its levels in parental and control siRNA-treated cells (Fig. 2C). These data indicate that CDX2 is involved in maintaining *MDR1* gene expression in gastrointestinal cell lines.

The 5′-flanking region of the *MDR1* gene contains a CDX2-responsive element

To identify potential CDX2-binding sites in the *MDR1* promoter region, genomic sequences immediately 5′ to the apparent transcription start site were searched, using a consensus-binding element for the Cdx A chicken caudal-related protein (5′-A, A/T, T, A/T, A, T, A/G-3′; ref. 23) and a previously described search algorithm (24). Four candidate CDX2-binding sites were found in the −4.0-kb region upstream of the presumptive transcription initiation sites: site A (5′-ATTTATG-3′, from −3,974 to −3,980), site B (5′-TTTTATG-3′, from −3,421 to −3,427), site C (5′-TTTTATG-3′, from −1,489 to −1,495), and site D (5′-ATTTATG-3′, from −1,463 to −1,469; Fig. 3A). To assess the role of these presumptive CDX2-binding sites in regulating *MDR1* transcription, several reporter gene constructs were generated (Fig. 3A). Reporter gene constructs containing 4.0 kb of a 5′-flanking sequence (−4,003/+50) from the *MDR1* gene showed strong activity in the HT29/PGS-CDX2 cell lines (Fig. 3B).

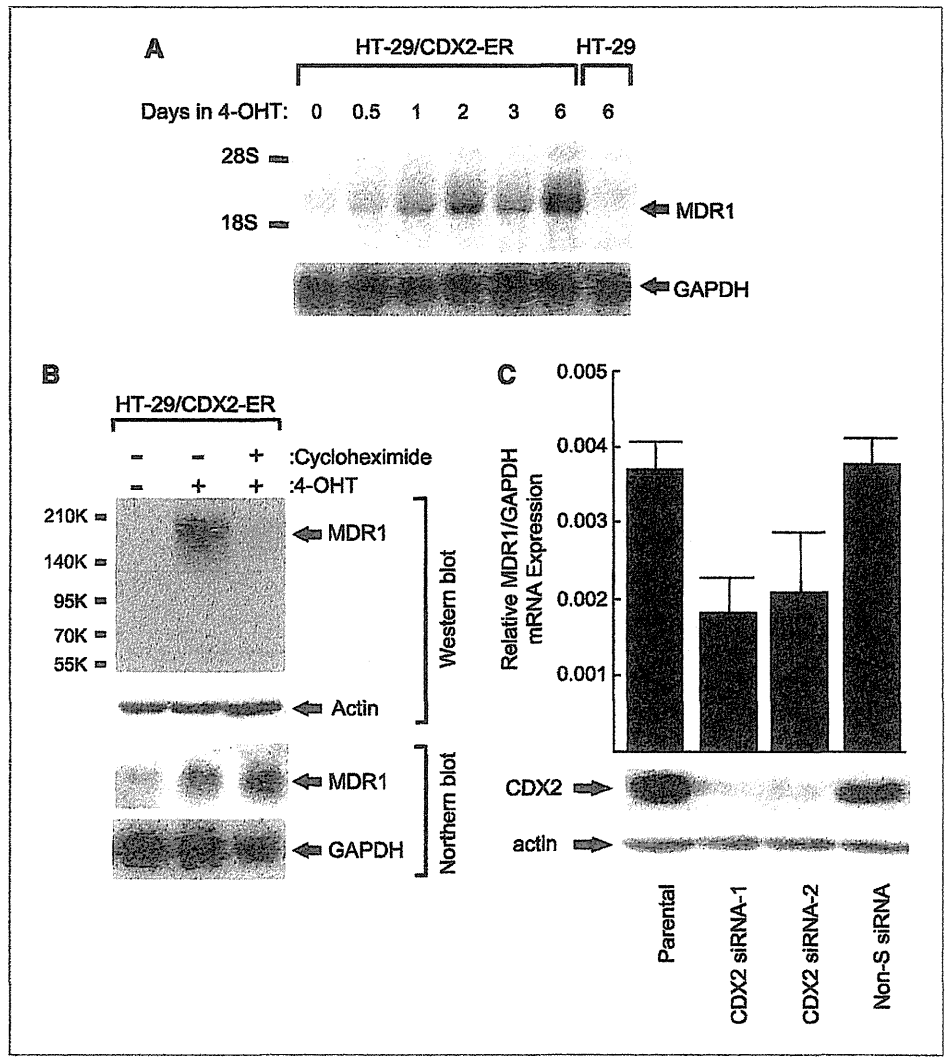

Figure 2. The *MDR1* gene is a primary target of CDX2 action. A, time course of *MDR1* gene induction in response to activation of a CDX2-ER fusion protein by 4-OHT. B, induction of *MDR1* transcript in response to activation of a CDX2-ER fusion protein by 4-OHT is not inhibited by the protein synthesis inhibitor cycloheximide, but protein synthesis is blocked. C, inhibition of CDX2 expression by siRNA targeting leads to decreased *MDR1* expression in CRC cell line DLD1. Assays were performed in triplicate; columns, mean; bars, SD.

Published OnlineFirst August 10, 2010; DOI:10.1158/0008-5472.CAN-09-4701

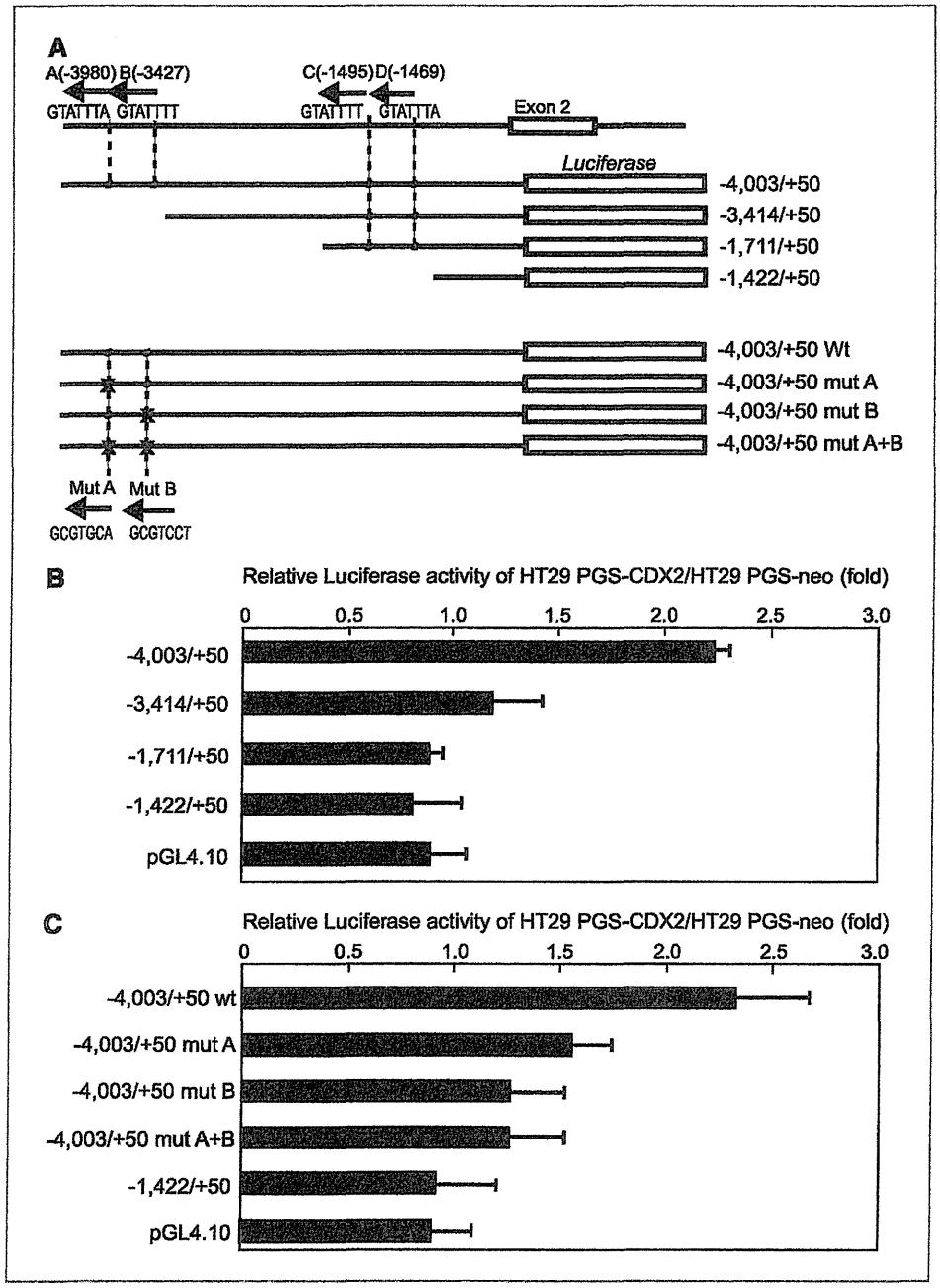

Figure 3. Localization of regulatory elements and CDX2 binding sites in the 5′-flanking region of the *MDR1* gene. A, schematic representation of the 5′-flanking region of the *MDR1* gene and *MDR1* reporter gene constructs. The location and sequence of four consensus CDX2-binding sites in the 5′-flanking region of *MDR1* are indicated. The direction of the arrows indicates the strand on which the candidate CDX2-binding element was found (i.e., sense or antisense). The *MDR1* genomic DNA sequences present in the reporter gene vectors are indicated. Localized mutations in the candidate CDX2-binding sites (i.e., site A and B) were introduced into the −4,003/+50 construct as noted (bottom), and the series of constructs generated is shown. B, key sequences for *MDR1* transcription in CDX2-expressing cell lines reside between bp −4,003 and −3,414. Columns, mean values of the luciferase activity ratio in HT29/PGS-CDX2 cells to that in HT29/PGS-neo cells; bars, SD. C, CDX2 candidate binding sites A and B play critical roles in *MDR1* transcription. All assays were performed in triplicate; columns, mean of luciferase activity ratio; bars, SD.

All the *MDR1* reporter gene constructs with deletions downstream of the 4.0-kb pair site showed decreased activity in HT29/PGS-CDX2 cell lines; thus, sequences between −3.4- and −4.0-kb pairs are important in activating *MDR1* transcription. Analysis of single and multiple mutations in the presumptive CDX2-binding sites in this region using HT29/PGS-CDX2 and HT29/PGS-neo showed that the presumptive CDX2-binding sites A and B play crucial roles in activating *MDR1* transcription (Fig. 3C).

CDX2 binds to elements in the 5′-flanking region of the *MDR1* gene

As previously noted, using the HT-29/CDX-ER cell line and the protein synthesis inhibitor cycloheximide, we found that the *MDR1* gene was a direct or primary target of CDX2. Additionally, *MDR1* reporter gene studies with localized mutations of CDX2-binding sites implied that CDX2 plays a major role in activating *MDR1* transcription by binding to one or more sites in the *MDR1* proximal promoter region. To confirm that CDX2 does indeed bind

Published OnlineFirst August 10, 2010; DOI:10.1158/0008-5472.CAN-09-4701

directly to sequences in the *MDR1* promoter region, we undertook ChIP assays using HT-29/CDX-ER cells. Before treatment of HT-29/CDX-ER cells with 4-OHT, the CDX2-ER fusion protein was expressed but remained inactive in the cells, likely because it was complexed with heat shock proteins. As would be predicted for cells lacking appreciable levels of functional CDX2, before 4-OHT treatment, we failed to recover DNA fragments of the promoter regions of *MDR1* in ChIP experiments with anti-CDX2 antibody (Fig. 4A). In contrast, on day 2 after 4-OHT–mediated activation of the CDX2-ER fusion protein, we readily recovered DNA fragments containing the *MDR1* promoter (Fig. 4A). The specificity of recovery of the *MDR1* promoter region following ChIP with anti-CDX2 antibody was shown by the fact that other irrelevant DNA fragments lacking CDX2-binding sites (e.g., exon 3 of the *CDX1* gene) were not recovered (Fig. 4A). Additionally, mock immunoprecipitation (mouse IgG whole molecule) yielded few *MDR1* or CDX1-specific DNA fragments (Fig. 4A). To confirm these data in endogenous CDX2, we performed the same ChIP assay in Caco2, CRC cell lines, which has strong endogenous CDX2 expression. We also recovered DNA fragments containing the MDR1 promoter region following ChIP with anti-CDX2 antibody (Fig. 4B). All these findings strongly suggest that CDX2 activates *MDR1* transcription by directly binding to sequences in the 5′-flanking region of the gene.

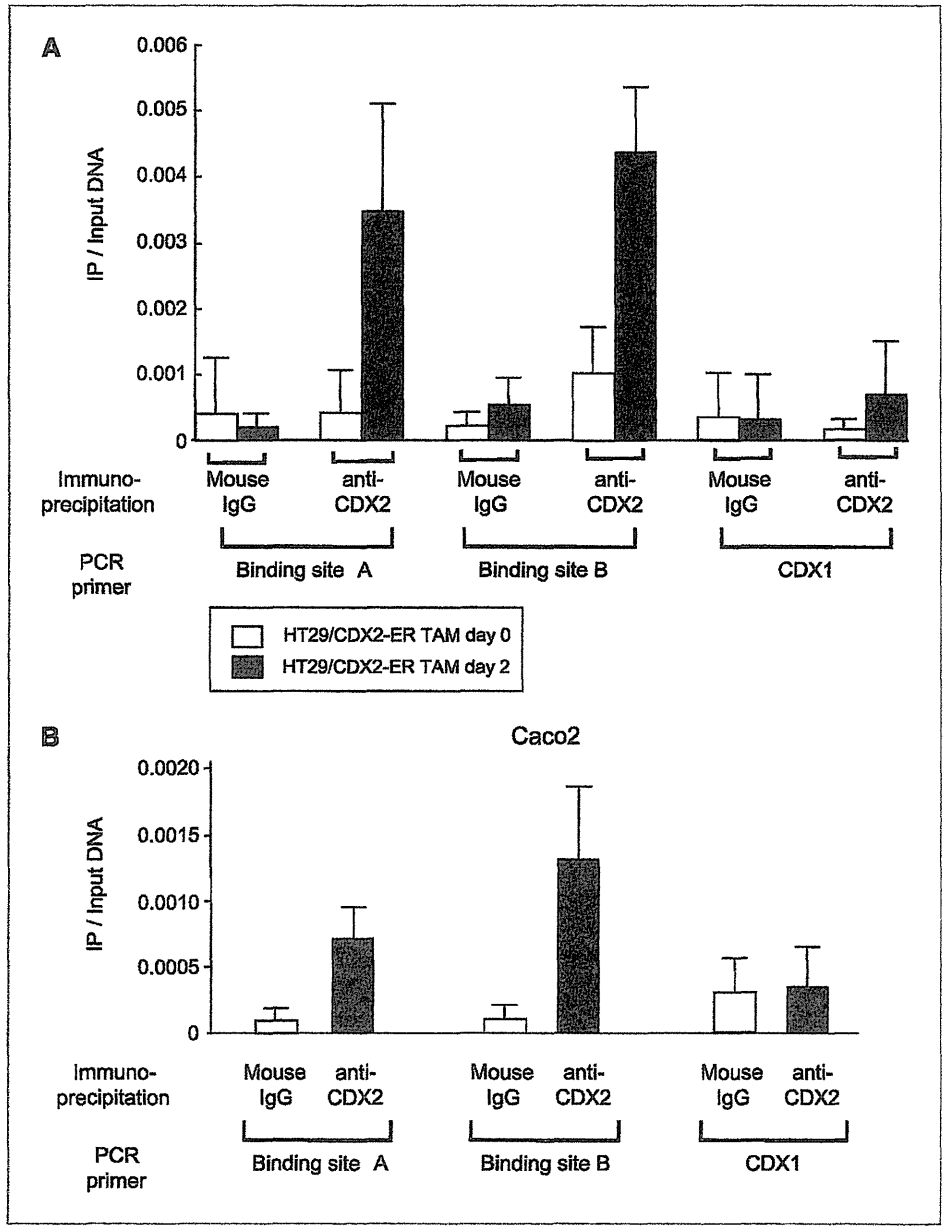

Figure 4. CDX2 binding to *MDR1* promoter region shown by ChIP. A, CDX2 function was activated in HT-29/CDX2-ER cells by treatment of the cells with 4-OHT, and the cells were harvested at the indicated time points. B, specificity of recovery of DNA fragments of MDR1 promoter region following ChIP with anti-CDX2 antibody was confirmed in Caco2, which has endogenous strong CDX2 expression. Assays were performed in triplicate, and mean and SD values are shown.

Published OnlineFirst August 10, 2010; DOI:10.1158/0008-5472.CAN-09-4701

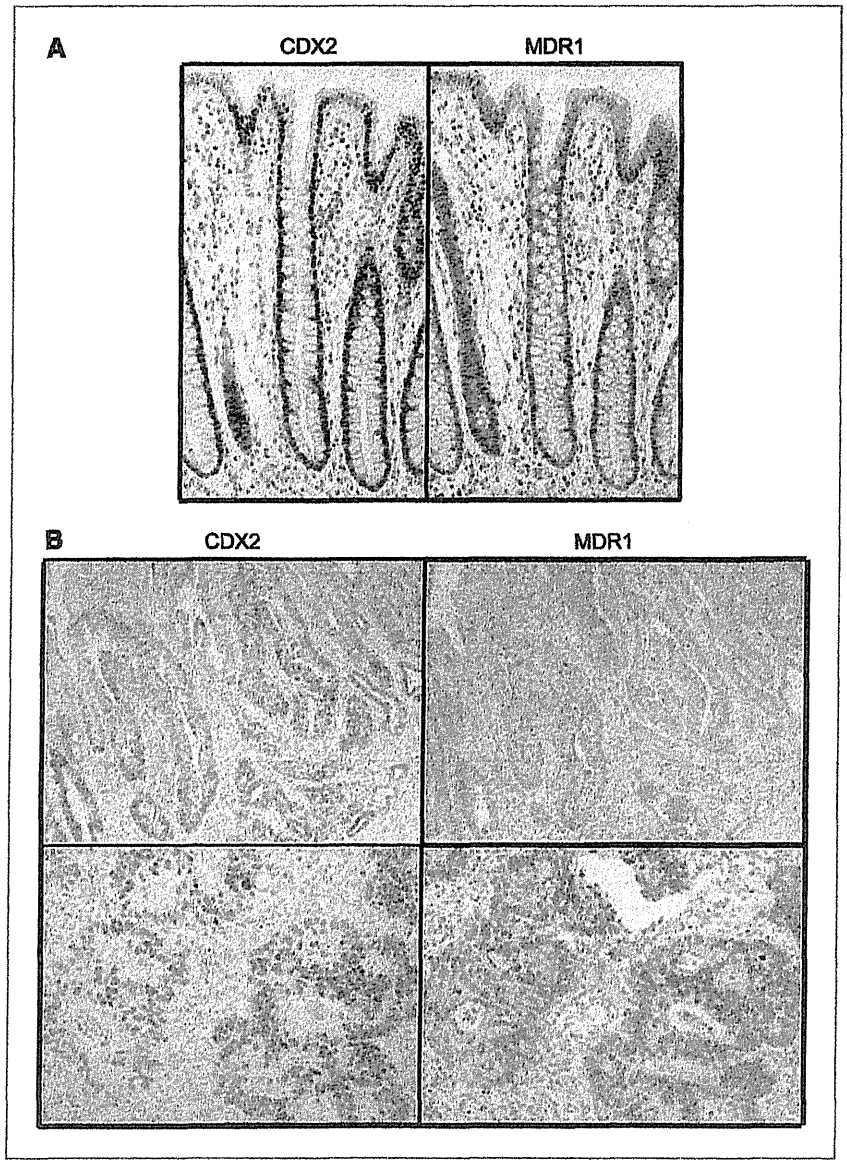

Figure 5. CDX2 and MDR1 expressions are well correlated in human colon epithelium and stomach cancer tissues. Immunohistochemistry was performed on formalin-fixed and paraffin-embedded tissues with anti-CDX2 monoclonal antibody (A and B, left) and with anti-MDR1 monoclonal antibody, C494 (A and B, right) in (A) human colon epithelium and (B) stomach cancer tissue.

CDX2 and MDR1 expression are tightly coupled in neoplastic tissues in the gastrointestinal tract

As previously noted, prior studies of CDX2 expression in normal adult tissues have shown strong CDX2 expression restricted to epithelial cells of the small intestine and colon, whereas *MDR1* is expressed in a broad range of normal tissues including epithelia of the liver; kidney; small and large intestine; and capillary endothelial cells in brain, ovary, and testis (25).

We examined the correlation between CDX2 and MDR1 expression in human healthy colon epithelium and CRC tissue microarray by immunohistochemical staining. Patterns of CDX2 and MDR1 expression are well correlated in normal colon epithelium (Fig. 5A). In CRC tissue microarray, we analyzed 302 CRC tissues. For statistical comparisons, moderate and high *MDR1* protein (P-glycoprotein) expression was evaluated against low MDR1 expression. In tissue microarray, 214 showed positive CDX2 expression (70.9%), whereas 201 showed positive MDR1 expression (66.6%). CDX2 and MDR1 expressions showed a strong positive correlation (Supplementary Table S1, $P < 0.001$). We then evaluated the correlation between CDX2 and MDR1 expression in stomach cancers because normal stomach epithelium shows low expression of both CDX2 and MDR1 (16, 26). CDX2 was stained intensely in nuclei of stomach cancer cells, whereas MDR1 was stained in the inner surface of neoplastic glands (Fig. 5B). Of 54 stomach cancers, 22 showed positive CDX2 expression (40.7%), whereas 25 showed positive MDR1 expression (46.3%). CDX2 and MDR1 expressions showed a strong positive correlation ($P < 0.001$; Supplementary Table S2).

Published OnlineFirst August 10, 2010; DOI:10.1158/0008-5472.CAN-09-4701

HT-29 cells ectopically expressing CDX2 have MDR1-dependent drug resistance

To determine whether MDR1 induced by CDX2 functions as a drug reflux pump, we analyzed the effects of chemotherapeutic drugs on HT-29/PGS-CDX2 and HT29/PGS-neo cells (Fig. 6A). The MDR1 nonsubstrates, that is, cisplatin, camptothecin, 5-fluorouracil, and doxorubicin, showed similar activity in HT-29/PGS-CDX2 and HT-29/PGS-neo cells, whereas the known MDR1 substrates (25), vincristine and paclitaxel, showed lesser activity [7.7- and 3.0-fold increase in IC_{50} (72 h), respectively] in HT-29/PGS-CDX2 cells (Fig. 6A).

To examine MDR1-dependent drug resistance, we conducted the same assay in the presence of the MDR1 inhibitor verapamil. Cotreatment with 2 μmol/L verapamil increased the activities of vincristine and paclitaxel in HT-29/PGS-CDX2 cells (Fig. 6B and C). Verapamil reduced the differences in the drug-induced cytotoxicity between HT-29/PGS-CDX2 and HT-29/PGS-neo cells (Fig. 6B and C). This suggests that increased resistance to vincristine and paclitaxel in HT-29/PGS-CDX2 cells is caused by overexpression of the *MDR1* gene.

Discussion

There is now a sizable body of data supporting the idea that the intestine-specific homeobox transcription factor CDX2 has a crucial role in directing intestinal epithelial development and differentiation (1, 2). However, the precise molecular mechanisms underlying tissue-specific expression of CDX2 and its downstream target genes remain undefined. To date, only a limited number of CDX2-regulated target genes have been suggested, including sucrase-isomaltase (27), glucagon (28), carbonic anhydrase 1 (29), calbindin-D9K (30), vitamin D receptor (31), lactase (32), guanylyl cyclase C (33), clusterin (34), gut-enriched Krüppel-like factor (35), heparin-binding epidermal growth factor–like growth factor (36), *MUC2* (37), LI-cadherin (16), *HEPH* (18), *Cdx2* itself through autoregulatory loop (38), insulin receptor substrate 2 (39), and solute carrier family 5, member 8 (SLC5A8; ref. 40).

In this study, we identified *MDR1* as a candidate gene directly regulated by CDX2. Evidence that CDX2 might regulate *MDR1* was initially obtained using high-density oligonucleotide microarrays to identify genes activated following overexpression of CDX2 in a CRC cell line showing very low endogenous CDX2 expression. Additionally, data indicating that endogenous *MDR1* expression was dependent on CDX2 were obtained, along with evidence that activation of CDX2 induced *MDR1* transcripts even in the presence of protein synthesis inhibitors. We identified four presumptive CDX2-binding sites in the 4-kb region upstream of the transcription start sites of *MDR1*. Reporter gene analysis showed that two of these elements were critical. Subsequent ChIP assays showed that CDX2 binds directly to this *MDR1* promoter region. Immunohistochemical staining analysis for 302 CRCs and 54 stomach cancers showed that CDX2 and MDR1 protein expressions were significantly correlated. Given the regulation of *MDR1* by CDX2 in neoplastic gastrointestinal tissues, CDX2, as well as MDR1, may be a useful marker for predicting the status of drug resistance in the stomach and perhaps elsewhere.

Although our data offer reliable support for the view that CDX2 plays a role in regulating *MDR1* transcription by binding to one or more elements in the proximal promoter region, CDX2 might not be sufficient for activating *MDR1* expression. It is possible that other factors along with CDX2 may be required to activate *MDR1* transcription in certain settings, such as in HT-29 cells, because two of the eight CDX2-positive CRC cell lines we studied (namely SW48 and LS174T) expressed very low or undetectable levels of *MDR1* transcripts and protein. Previously, we obtained similar evidence that CDX2 was required but not sufficient for activating *LI-cadherin* and *HEPH* transcription (16, 18). On the other hand, our data indicated that inhibition of CDX2 expression by siRNA leads to decreased *MDR1* transcription, suggesting that CDX2 does play a key role in maintaining *MDR1* expression in certain settings, such as in CDX2- and MDR1-expressing CRC cells. It will be interesting in the future to define other factors that cooperate with CDX2 in regulating *MDR1*, LI-cadherin, and HEPH expression in gastrointestinal tissues.

In our study, we showed that expression of CDX2 induced MDR1-dependent drug resistance in a CRC cell line, which was reversed by the MDR1-specific inhibitor verapamil (21), suggesting a role of CDX2 in the regulation of *MDR1* gene expression in drug resistance. Consistent with the intestine-specific expression of CDX2 in humans and mice, recent analysis for tissue-specific murine *Mdr1a* gene expression in naïve animals revealed that the basal *Mdr1a* expression level was 100-fold higher in the intestine than in other *MDR1*-expressing tissues such as the liver, kidney, and spleen (25, 41). In epithelial cells of the lower gastrointestinal tract (jejunum, ileum, and colon), high levels of MDR1 protein are found only on the apical surfaces of superficial columnar epithelial cells, which suggests a function to prevent uptake of substrates and perhaps to facilitate excretion across the mucosa of the gastrointestinal tract (26). Given the role of CDX2 in the establishment and maintenance of intestinal epithelium, CDX2 may play a critical role in protecting the intestinal epithelium and the human body from toxic xenobiotics by stably inducing *MDR1* even under naïve conditions.

In cancer tissue, the *MDR1* gene was originally identified as an overexpressed and amplified gene in multiple drug-resistant cells (19, 25). The *MDR1* gene encodes P-glycoprotein, a member of the large ATP-binding cassette superfamily of transmembrane proteins (ATP-binding cassette, sub family B, member 1) that transports structurally different hydrophobic chemotherapeutic agents outward in an energy-dependent manner. Regulation of *MDR1* gene expression is complex because like many TATA-less promoters (42), the promoter of the *MDR1* gene contains multiple start sites. In studies of CRCs, expression of *MDR1* was correlated with pathologic grading of tumors, being most intense in well-differentiated tumors and low in poorly differentiated ones (43). Similarly, moderately differentiated gastric carcinomas expressed a higher level of MDR1 than poorly differentiated

Published OnlineFirst August 10, 2010; DOI:10.1158/0008-5472.CAN-09-4701

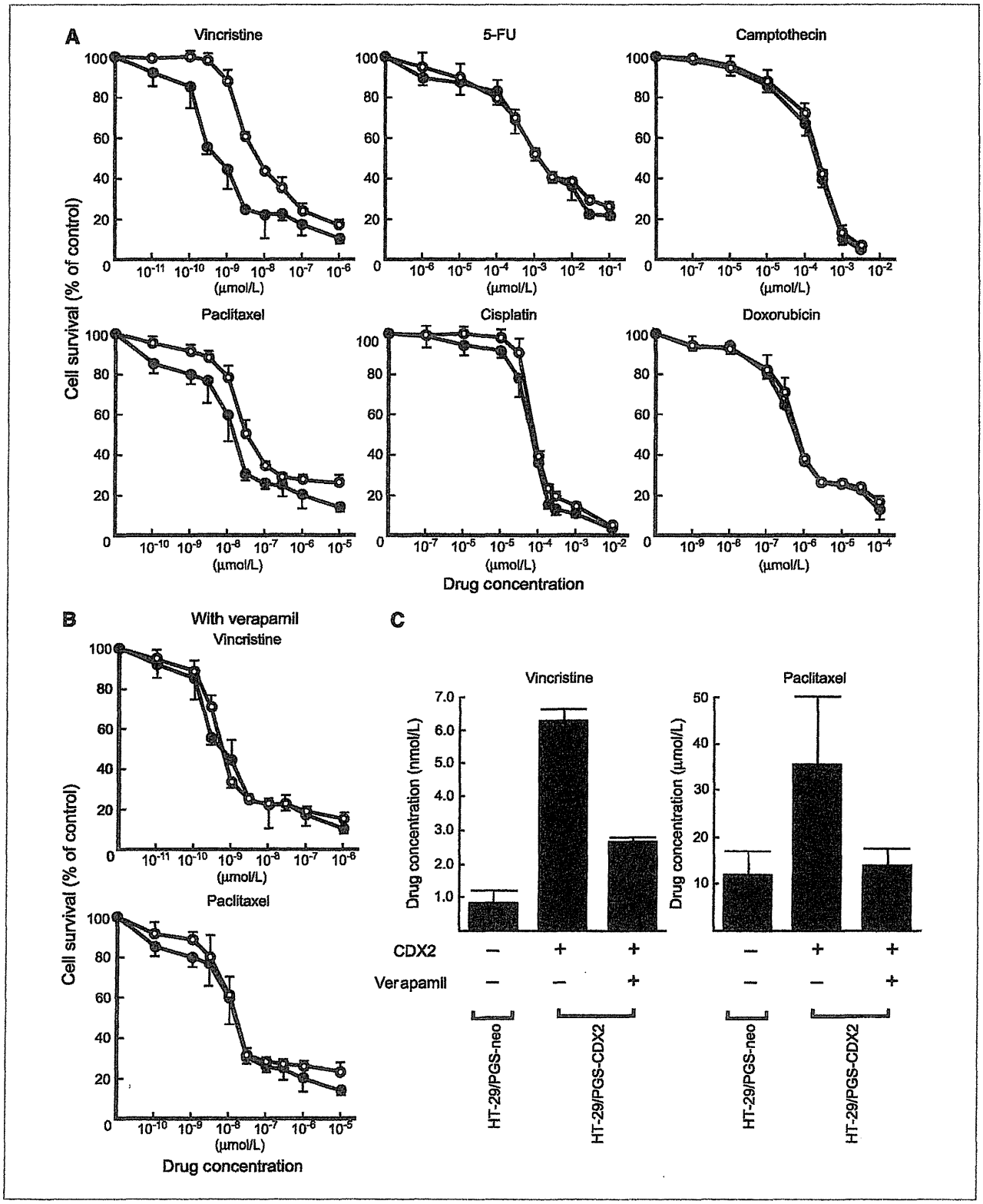

Figure 6. HT29 cells ectopically expressing CDX2 have MDR1-dependent drug resistance. A, effect of chemotherapeutic drugs on HT29/PGS-CDX2 (○) and HT29/PGS-neo (●) cell lines. B, effect of additional verapamil on vincristine and paclitaxel in HT29/PGS-CDX2 (○) and HT29/PGS-neo (●) cell lines. C, [IC_{50} (72 h)] determined by MTT assay on HT29/PGS-CDX2 and HT29/PGS-neo cells. Cotreatment with verapamil significantly recovered the sensitivity of vincristine and paclitaxel on HT-29/PGS-CDX2 cells. The cytotoxic assays were performed in triplicate; points, mean; bars, SD.

Published OnlineFirst August 10, 2010; DOI:10.1158/0008-5472.CAN-09-4701

ones (44). Although studies of CRCs arising in humans have not offered definitive proof of a causal role for CDX2 inactivation in the cancer process, it is quite clear that loss of CDX2 expression is seen in a subset of primary CRCs, particularly tumors with minimal differentiation (45). Consistent with our previous observation in large cell minimally differentiated adenocarcinoma of the colon, recent multivariate analysis also indicates that loss of CDX2 expression is associated with less-differentiated carcinoma and advanced stage, although CDX2 loss is not independently associated with patient survival (15, 46). Considering the roles of CDX2 in promoting cellular differentiation and inhibiting proliferation (45), CDX2 loss could conceivably contribute to aggressive tumor behavior, although MDR1 loss induced by CDX2 suppression may have some beneficial influence on patient survival with reduced drug resistance.

In conclusion, our findings implicating CDX2 in regulation of *MDR1* offer data on specific factors and mechanisms regulating MDR1 expression in gastrointestinal cancers. However, several outstanding issues regarding the transcriptional regulation of *MDR1* by CDX2 remain to be addressed. Due to the complexity of the mechanism of drug resistance, further studies of *MDR1* and its regulation by CDX2 in various gastrointestinal cancers should help to enhance understanding of the mechanism of aberrant (ectopic) expression of CDX2 and its downstream target *MDR1*, and in the development of a strategy to select chemotherapy regimens based on the status of CDX2 and *MDR1* expression.

Disclosure of Potential Conflicts of Interest

No potential conflicts of interest were disclosed.

Acknowledgments

We thank Drs. Hideki Yamamoto and Yoshitaka Tomoda for their advice, Yuko Ishida and Midori Kiyokawa for their expert technical assistance, and the Analysis Center of Life Science, Hiroshima University, for the use of their facilities.

Grant Support

US NIH grants CA082223. NIH R01CA082223 (E.R. Fearon).
The costs of publication of this article were defrayed in part by the payment of page charges. This article must therefore be hereby marked *advertisement* in accordance with 18 U.S.C. Section 1734 solely to indicate this fact.

Received 12/30/2009; revised 05/27/2010; accepted 06/11/2010; published OnlineFirst 08/10/2010.

References

1. Silberg DG, Swain GP, Suh ER, Traber PG. Cdx1 and cdx2 expression during intestinal development. Gastroenterology 2000;119:961–71.
2. Beck F. The role of Cdx genes in the mammalian gut. Gut 2004;53: 1394–6.
3. Moreno E, Morata G. Caudal is the Hox gene that specifies the most posterior Drosophile segment. Nature 1999;400:873–7.
4. Macdonald PM, Struhl G. A molecular gradient in early *Drosophila* embryos and its role in specifying the body pattern. Nature 1986; 324:537–45.
5. Niwa H, Toyooka Y, Shimosato D, et al. Interaction between Oct3/4 and Cdx2 determines trophectoderm differentiation. Cell 2005;123: 917–29.
6. Tolkunova E, Cavaleri F, Eckardt S, et al. The caudal-related protein cdx2 promotes trophoblast differentiation of mouse embryonic stem cells. Stem Cells 2006;24:139–44.
7. Chawengsaksophak K, James R, Hammond VE, Kontgen F, Beck F. Homeosis and intestinal tumours in Cdx2 mutant mice. Nature 1997; 386:84–7.
8. Tamai Y, Nakajima R, Ishikawa T, Takaku K, Seldin MF, Taketo MM. Colonic hamartoma development by anomalous duplication in Cdx2 knockout mice. Cancer Res 1999;59:2965–70.
9. Bonhomme C, Duluc I, Martin E, et al. The Cdx2 homeobox gene has a tumour suppressor function in the distal colon in addition to a homeotic role during gut development. Gut 2003;52:1465–71.
10. Aoki K, Tamai Y, Horiike S, Oshima M, Taketo MM. Colonic polyposis caused by mTOR-mediated chromosomal instability in Apc+/Δ716 Cdx2+/– compound mutant mice. Nat Genet 2003; 35:323–30.
11. Beck F, Chawengsaksophak K, Waring P, Playford RJ, Furness JB. Reprogramming of intestinal differentiation and intercalary regeneration in Cdx2 mutant mice. Proc Natl Acad Sci U S A 1999;96: 7318–23.
12. Silberg DG, Sullivan J, Kang E, et al. Cdx2 ectopic expression induces gastric intestinal metaplasia in transgenic mice. Gastroenterology 2002;122:689–96.
13. Mutoh H, Hakamata Y, Sato K, et al. Conversion of gastric mucosa to intestinal metaplasia in Cdx2-expressing transgenic mice. Biochem Biophys Res Commun 2002;294:470–9.
14. Ee HC, Erler T, Bhathal PS, Young GP, James RJ. Cdx-2 homeodomain protein expression in human and rat colorectal adenoma and carcinoma. Am J Pathol 1995;147:586–92.
15. Hinoi T, Tani M, Lucas PC, et al. Loss of CDX2 expression and microsatellite instability are prominent features of large cell minimally differentiated carcinomas of the colon. Am J Pathol 2001;159: 2239–48.
16. Hinoi T, Lucas PC, Kuick R, Hanash S, Cho KR, Fearon ER. CDX2 regulates liver intestine-cadherin expression in normal and malignant colon epithelium and intestinal metaplasia. Gastroenterology 2002; 123:1565–77.
17. Eda A, Osawa H, Yanaka I, et al. Expression of homeobox gene CDX2 precedes that of CDX1 during the progression of intestinal metaplasia. J Gastroenterol 2002;37:94–100.
18. Hinoi T, Gesina G, Akyol A, et al. CDX2-regulated expression of iron transport protein hephaestin in intestinal and colonic epithelium. Gastroenterology 2005;128:946–61.
19. Pastan I, Gottesman MM. Multidrug resistance. Annu Rev Med 1991; 42:277–86.
20. Littlewood TD, Hancock DC, Danielian PS, Parker MG, Evan GI. A modified oestrogen receptor ligand-binding domain as an improved switch for the regulation of heterologous proteins. Nucleic Acids Res 1995;23:1686–90.
21. Tsuruo T, Iida H, Tsukagoshi S, Sakurai Y. Overcoming of vincristine resistance in P388 leukemia *in vivo* and *in vitro* through enhanced cytotoxicity of vincristine and vinblastine by verapamil. Cancer Res 1981;41:1967–72.
22. Mallo GV, Soubeyran P, Lissitzky JC, et al. Expression of the Cdx1 and Cdx2 homeotic genes leads to reduced malignancy in colon cancer-derived cells. J Biol Chem 1998;273:14030–6.
23. Margalit Y, Yarus S, Shapira E, Gruenbaum Y, Fainsod A. Isolation and characterization of target sequences of the chicken CdxA homeobox gene. Nucleic Acids Res 1993;21:4915–22.
24. Heinemeyer T, Wingender E, Reuter I, et al. Databases on transcriptional regulation: TRANSFAC, TRRD and COMPEL. Nucleic Acids Res 1998;26:362–7.
25. Ambudkar SV, Dey S, Hrycyna CA, Ramachandra M, Pastan I, Gottesman MM. Biochemical, cellular, and pharmacological aspects of the multidrug transporter. Annu Rev Pharmacol Toxicol 1999;39:361–98.

Published OnlineFirst August 10, 2010; DOI:10.1158/0008-5472.CAN-09-4701

26. Thiebaut F, Tsuruo T, Hamada H, Gottesman MM, Pastan I, Willingham MC. Cellular localization of the multidrug-resistance gene product P-glycoprotein in normal human tissues. Proc Natl Acad Sci U S A 1987;84:7735–8.
27. Suh E, Chen L, Taylor J, Traber PG. A homeodomain protein related to caudal regulates intestine-specific gene transcription. Mol Cell Biol 1994;14:7340–51.
28. Jin T, Trinh DK, Wang F, Drucker DJ. The caudal homeobox protein cdx-2/3 activates endogenous proglucagon gene expression in InR1–9 islet cells. Mol Endocrinol 1997;11:203–9.
29. Drummond FJ, Sowden J, Morrison K, Edwards YH. Colon carbonic anhydrase 1: transactivation of gene expression by the homeodomain protein Cdx2. FEBS Lett 1998;423:218–22.
30. Colnot S, Romagnolo B, Lambert M, et al. Intestinal expression of the calbindin-D9K gene in transgenic mice. Requirement for a Cdx2-binding site in a distal activator region. J Biol Chem 1998;273:31939–46.
31. Yamamoto H, Miyamoto K, Li B, et al. The caudal-related homeodomain protein Cdx-2 regulates vitamin D receptor gene expression in the small intestine. J Bone Miner Res 1999;14:240–7.
32. Fang R, Santiago NA, Olds LC, Sibley E. The homeodomain protein Cdx2 regulates lactase gene promoter activity during enterocyte differentiation. Gastroenterology 2000;118:115–27.
33. Park J, Schulz S, Waldman SA. Intestine-specific activity of the human guanylyl cyclase C promoter is regulated by Cdx2. Gastroenterology 2000;119:89–96.
34. Suh E, Wang Z, Swain GP, Tenniswood M, Traber PG. Clusterin gene transcription is activated by caudal-related homeobox genes in intestinal epithelium. Am J Physiol Gastrointest Liver Physiol 2001;280:G149–56.
35. Dang DT, Mahatan CS, Dang LH, Agboola IA, Yang VW. Expression of the gut-enriched Kruppel-like factor (Kruppel-like factor 4) gene in the human colon cancer cell line RKO is dependent on CDX2. Oncogene 2001;20:4884–90.
36. Uesaka T, Lu H, Katoh O, Watanabe H. Heparin-binding EGF-like growth factor gene transcription regulated by Cdx2 in the intestinal epithelium. Am J Physiol Gastrointest Liver Physiol 2002;283:G840–7.
37. Yamamoto H, Bai YQ, Yuasa Y. Homeodomain protein CDX2 regulates goblet-specific MUC2 gene expression. Biochem Biophys Res Commun 2003;300:813–8.
38. Xu F, Li H, Jin T. Cell type-specific autoregulation of the Caudal-related homeobox gene Cdx-2/3. J Biol Chem 1999;274:34310–6.
39. Modica S, Morgano A, Salvatore L, et al. Expression and localisation of insulin receptor substrate 2 in normal intestine and colorectal tumours. Regulation by intestine-specific transcription factor CDX2. Gut 2009;58:1250–9.
40. Kakizaki F, Aoki K, Miyoshi H, Carrasco N, Aoki M, Taketo MM. CDX transcription factors positively regulate expression of solute carrier family 5, member 8 in the colonic epithelium. Gastroenterology 2010;138:627–35.
41. Gu L, Tsark WM, Brown DA, Blanchard S, Synold TW, Kane SE. A new model for studying tissue-specific mdr1a gene expression *in vivo* by live imaging. Proc Natl Acad Sci U S A 2009;106:5394–9.
42. Labialle S, Gayet L, Marthinet E, Rigal D, Baggetto LG. Transcriptional regulators of the human multidrug resistance 1 gene: recent views. Biochem Pharmacol 2002;64:943–8.
43. Potocnik U, Ravnik-Glavac M, Golouh R, Glavac D. Naturally occurring mutations and functional polymorphisms in multidrug resistance 1 gene: correlation with microsatellite instability and lymphoid infiltration in colorectal cancers. J Med Genet 2002;39:340–6.
44. Mizoguchi T, Yamada K, Furukawa T, et al. Expression of the MDR1 gene in human gastric and colorectal carcinomas. J Natl Cancer Inst 1990;82:1679–83.
45. Hinoi T, Loda M, Fearon ER. Silencing of CDX2 expression in colon cancer via a dominant repression pathway. J Biol Chem 2003;278:44608–16.
46. Baba Y, Nosho K, Shima K, et al. Relationship of CDX2 loss with molecular features and prognosis in colorectal cancer. Clin Cancer Res 2009;15:4665–73.

Original Paper

Pathobiology

Pathobiology 2010;77:241–248
DOI: 10.1159/000314966

Received: March 2, 2010
Accepted after revision: May 11, 2010

Upregulation of Connexin 30 in Intestinal Phenotype Gastric Cancer and Its Reduction during Tumor Progression

Kazuhiro Sentani[a] Naohide Oue[a] Naoya Sakamoto[a] Katsuhiro Anami[a]
Yutaka Naito[a] Kazuhiko Aoyagi[b] Hiroki Sasaki[b] Wataru Yasui[a]

[a]Department of Molecular Pathology, Hiroshima University Graduate School of Biomedical Sciences, Hiroshima, and [b]Genetics Division, National Cancer Center Research Institute, Tokyo, Japan

Key Words
Gastric cancer · Intestinal phenotype · Connexin 30 · Microarray

Abstract
Aims: The mucin phenotype is associated with clinicopathological findings and tumorigenesis in gastric cancer (GC). The aim was to search for a novel marker regulating the intestinal phenotype of GC. ***Methods and Results:*** We performed microarray analyses, and *GJB6* (encoding connexin 30) was identified as a gene associated with the intestinal phenotype. Immunostaining of connexin 30 in 169 GC cases revealed that 47 (28%) cases were positive for connexin 30, while connexin 30 was negative in nonneoplastic gastric tissue. Connexin 30-negative GC cases showed more advanced T grade, N grade, and tumor stage than connexin 30-positive GC cases. Six (13%) GC cases positive for connexin 30 were histologically of the differentiated type. In addition, the expression of gastric and intestinal phenotypes of GC was examined by immunostaining for MUC5AC, MUC6, MUC2, and CD10. Connexin 30 expression occurred more frequently in the intestinal phenotype (48%) than in other phenotypes (21%) of GC. ***Conclusion:*** These results indicate that the expression of connexin 30 is a novel differentiation marker mediating the biological behavior of intestinal phenotype GC.

Introduction

According to the World Health Organization, gastric cancer (GC) is the fourth most common malignancy worldwide, with approximately 870,000 new cases occurring yearly. Mortality due to GC is second only to that due to lung cancer [1]. Cancer develops as a result of multiple genetic and epigenetic alterations [2, 3]. Better knowledge of the changes in gene expression that occur during gastric carcinogenesis may lead to improvements in diagnosis, treatment, and prevention. Identification of novel biomarkers for cancer diagnosis and novel targets for treatment are major goals in this field [4]. Array-based hybridization [5] and serial analysis of gene expression (SAGE) [6] are currently the most common approaches used to identify potential molecular markers for cancer.

GCs have been classified into 2 histological types: an intestinal type and a diffuse type by Lauren [7], or a differentiated type and an undifferentiated type by Nakamura et al. [8], based on the tendency toward gland formation. It has been suggested that these 2 types involve distinct pathways during carcinogenesis [7–10]. Recent studies have demonstrated that GCs are also classified as having a gastric, gastric and intestinal mixed, or intestinal phenotype depending on the expression of mucin phenotypic markers [11–18]. The mucin expression and phenotype of tumors are associated with clinicopatho-

KARGER
Fax +41 61 306 12 34
E-Mail karger@karger.ch
www.karger.com

1015–2008/10/0775–0241$26.00/0

Accessible online at:
www.karger.com/pat

Wataru Yasui, MD, PhD
Department of Molecular Pathology
Hiroshima University Graduate School of Biomedical Sciences
1-2-3 Kasumi, Minami-ku, Hiroshima 734-8551 (Japan)
Tel. +81 82 257 5145, Fax +81 82 257 5149, E-Mail wyasui@hiroshima-u.ac.jp